Magnetic Design of Relays

By R. L. PEEK, Jr., and H. N. WAGAR

(Manuscript received September 24, 1953)

The mechanical work and the speed of operation of telephone relays are determined in a large measure by the characteristics of the relay magnet. The underlying magnetic principles and the resulting design relationships for magnets are discussed in this article, which is in part a review of the background material and in part a description of its use in developing methods for magnet design and the analysis of magnet performance.

Basic energy considerations are shown to determine the relations between the work capacity and the magnetization characteristics, and analytical expressions for the latter are given in terms of the dimensions and materials of the magnet. These expressions are developed for the magnetic circuit approximation to static field theory, which is shown to provide an adequate representation of the field relations controlling performance. Methods are given for representing the magnetic circuit relations by means of a simple equivalent circuit. Expressions are derived for the mechanical output of the relay in parameters of this simple equivalent circuit, and these expressions used to determine optimum conditions for meeting specific design objectives.

INTRODUCTION

The complex switching equipment which handles the telephone traffic in automatic central offices is built up of simple component elements, of which the great majority are telephone relays. The large investment in these relays, of which tens of millions are made each year, has led to intensive effort to construct and use them as cheaply as possible, so that they will perform their function at a minimum over-all cost to the telephone system and thus to the subscriber. As the costs of use vary with the efficiency and speed, maximum economy requires the solution of technical problems in magnet design as well as the related problems of mechanical design for economy in manufacture. As a result, the technology of magnet design is under constant study at Bell Telephone Laboratories, directed to increased understanding of magnet performance

and to its improvement. This article gives the background of this technology as it applies to the dc telephone relay.

A telephone relay is an electromagnetic switch which actuates metallic contacts in response to signals applied to its coil. Its characteristics as a component of switching circuits are defined primarily by (1) the contact assembly, (2) the coil resistance, (3) the current flow requirements for operation, holding, and release, and (4) the operate and release times. The design of the contact assembly determines the number and nature of the contacts, the sequence of their operation, their current carrying capacity, and their reliability and life.

Structurally, the design of the relay, including both the electromagnet and the contact assembly, is governed not only by the performance requirements but also by the manufacturing considerations which determine the relay's initial cost, and by equipment considerations relating to the way it is mounted, wired, adjusted, and maintained. The ultimate objective is to perform a circuit function at a minimum over-all cost, including the costs of installation, power consumption, maintenance and replacement, as well as initial cost.

The design of the contact assembly determines a force-displacement characteristic representing the mechanical work which must be done by the electromagnet. The relations between this mechanical output and the electrical input to the coil are determined by the magnetic design of the relay, or specifically of its electromagnet. The electromagnetic design is therefore subject to the performance requirements, to the design of the contact assembly, and to the manufacturing and equipment considerations applying to the whole relay.

Magnetic design thus requires the ability to determine the effect on the performance of alternative choices of the configuration, dimensions, and materials of the electromagnet, of alternative load characteristics corresponding to variations in the design of the contact assembly, and of alternatives with respect to the coil dimensions and characteristics. The basic relations required for such prediction of performance are the magnetization relations, which express the field strength of the electromagnet as a function of the ampere turns, and the armature position.

The present article describes the evaluation of magnetization relations, and their use in relating the mechanical output with the electrical input to the coil. The time required for operation, which also depends upon the magnetization relations, is discussed in a separate article.[1] While much of the material given here has a broader application, the discussion of its use will be confined to the case of the simple neutral (non-polar) relay.

To illustrate the objectives of magnetic design, reference may be made to Fig. 1, which shows the load characteristic of the recently developed general purpose wire spring relay for a particular contact arrangement. The figure is taken from an article[2] describing this relay, which discusses the economic and other considerations which governed its design. Included in the figure are curves showing the pull exerted by this relay's magnet for various values of coil ampere turns. These pull curves determine the ampere turns required to operate a contact arrangement having a specific load characteristic, such as that shown. By means of the magnetization relations, these pull characteristics can be related to the design of the electromagnet.

The notation used in this article conforms to the list that is given on page 257.

1 THE COIL CONSTANT

The relay coil characteristics of interest in its use as a circuit component are its resistance and the current flow for operation. Subject to some qualifications as to available voltages and wire sizes, these may be summarized in a statement of the steady state power I^2R supplied in operation. As illustrated in Fig. 1, the coil quantity determined jointly by the load and the magnetic design is the ampere turn value NI. The power and the ampere turn value are related by the coil constant G_c or N^2/R (which equals $(NI)^2/(I^2R)$). This quantity is the equivalent single turn conductance of the coil, and is usually expressed in mhos. It is determined by the coil dimensions, as can be shown as follows:

Let A be the area of a cross-section of the coil as cut by a plane through the coil axis. Let m be the mean length of turn, the arithmetic mean of the lengths of the inner and outer turns. Then the coil volume S equals Am. If a is the cross-section of the wire, the number of turns N equals eA/a, where e is the copper efficiency, or fraction of the coil volume occupied by conductor. Substituting S/m for A, N equals $eS/(am)$. The wire length is Nm, and hence the resistance R equals $\rho Nm/a$, where ρ is the resistivity of the conductor. Hence N/R equals $a/(m\rho)$, and the coil constant is given by:

$$G_c = \frac{N^2}{R} = \frac{eS}{\rho m^2}. \tag{1}$$

The coil constant is thus independent of the wire size, except to the minor extent that the copper efficiency e decreases as the wire is made finer. With this qualification, and assuming copper wire to be used, the

coil constant is wholly determined by the coil dimensions and the type of insulation used. Thus the power required for relay operation depends upon (1) the load characteristic of the contact arrangement, (2) the magnetic characteristics which relate the pull to the ampere turns, and (3) the coil dimensions as defined by S/m^2, which determines the coil constant N^2/R, and thus the relation between ampere turns and power input.

The external dimensions of relays are largely determined by the coil

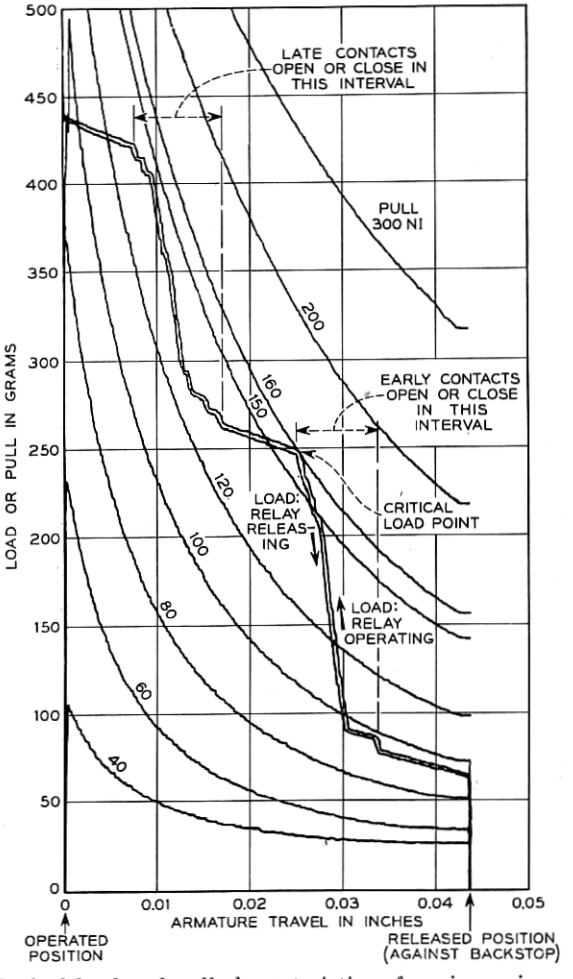

Fig. 1 — Typical load and pull characteristics of a wire spring relay with 12 transfer contacts.

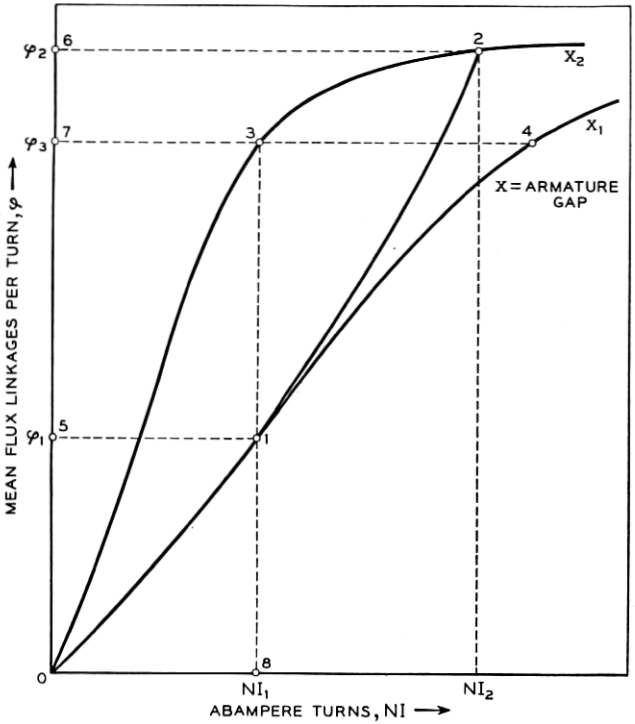

Fig. 2 — Energy relations in magnetization.

size, or winding space provided. The choice of these dimensions reflects an economic balance between the manufacturing costs of the magnet and its coil, which increase with these dimensions, and the savings in power cost resulting from increasing the coil constant.

2 MAGNETIZATION RELATIONS

The magnetization relations of an electromagnet define the steady state flux linkages of the coil as a function of the two variables: magnetomotive force $\mathfrak{F}$ (equal to $4\pi NI$), and the gap x, which specifies the armature position. They may be represented by a family of curves each giving the average flux linked per turn plotted against NI for a particular value of x. In Fig. 2, the curves marked x_1 and x_2 represent two such curves, where x_2 corresponds to a smaller gap than x_1.

To determine how the magnetization relations depend upon the dimensions and configuration of the electromagnet requires their interpretation in terms of static field theory. Such interpretation is needed in deter-

mining the design conditions for attaining a desired performance. For a specific structure, however, the observed magnetization relations, apart from any other interpretation, provide a record of the part of the electrical energy input to the coil which is stored in the electromagnet. The performance of the magnet with respect to the mechanical work which this stored energy can do may be determined directly from the way in which this energy varies with armature position. The experimental determination of the flux φ for particular values of NI and x involves a measurement of the electrical quantity $N\varphi$ defined by the equation:

$$N\varphi = \int_{i=0}^{i=I} (E - iR)\, dt. \tag{2}$$

The electrical energy U stored in making this measurement is the time integral of $i(E - iR)$, or:

$$U = \int_{i=0}^{i=I} (E - iR)i\, dt = \int_{0}^{N\varphi} i\, d(N\varphi).$$

Hence a plot of $N\varphi$ versus I gives a measure of the stored energy U represented by the area between the curve and the axis of $N\varphi$. This conclusion is quite independent of any physical meaning attached to $N\varphi$ other than the definition of equation (2). Plotting φ versus NI, rather than $N\varphi$ versus I, is merely a change of scale, which does not affect the value of the area measuring the stored energy U. It is convenient to make this change of scale because the relation between φ and NI is independent of the number of turns N, provided the location and dimensions of the coil are unchanged. The preceding expression for U may therefore be written as:

$$U = \int_{0}^{\varphi} Ni\, d\varphi. \tag{3}$$

Thus for $NI = NI_1$ in Fig. 2, U is measured by the area 0–1–5 for $x = x_1$, and by the area 0–3–7 for $x = x_2$.

Magnetization curves have the general character shown in Fig. 2. They are approximately linear for small values of φ, but at higher values bend over and approach a limiting value, φ''. This limiting value is the saturation flux, determined by the material and dimensions of the electromagnet, and designated throughout this paper by the double prime superscript.

The ratio of the magnetomotive force $\mathfrak{F}$ to the flux φ is the reluctance $\mathfrak{R}$, as defined by the equation:

$$\mathfrak{F} = 4\pi NI = \mathfrak{R}\varphi. \tag{4}$$

Over the linear portion of a magnetization curve, $\mathfrak{R}$ is a function of x only, or a constant for a particular curve. In this case, integration of equation (3) gives the following alternative expressions for the field energy U:

$$U = \frac{2\pi(NI)^2}{\mathfrak{R}} = \frac{\mathfrak{R}\varphi^2}{8\pi} = \frac{NI\varphi}{2}. \tag{5}$$

Over the upper curved portions of a magnetization curve, $\mathfrak{R}$ is a function of φ as well as of x, and equations (5) do not apply.

Decreasing Magnetization

In relay terminology, "operation," following closure of the coil circuit, is distinguished from "release," which follows opening of the circuit. The preceding discussion applies directly to the relations for increasing magnetization, as in operation. In release, the field energy and the current decrease together, giving a decrease in $N\varphi$ measured by a voltage time integral similar to the right-hand side of equation (2), but of opposite sign. The resulting decreasing magnetization curve is obtained by subtracting the decrease in $N\varphi$ from its initial value. The decreasing magnetization curve is higher than the magnetization curve, and the field energy recovered electrically is correspondingly less than that stored in magnetization; the difference corresponds to the loss of energy through hysteresis in the magnetic material.

Mechanical Output

Referring to Fig. 2, let the current have the steady value I_1, with the armature at rest at x_1. If the current increases to I_2 while the armature moves from x_1 to x_2, the flux φ varies with Ni along some curve such as 1–2 corresponding to the values of x and Ni concurrently attained. The electrical energy drawn by the coil in this process (aside from the heating loss) is given by the integral of $i\,d(N\varphi)$, or $Ni\,d\varphi$, taken along the curve 1–2. Part of this energy appears in the increase in the field energy from U_1 to U_2 as given by equation (3) for the points 1 and 2 respectively. The balance represents the mechanical work done, the integral of Fdx from x_1 to x_2 where F is the pull. Hence:

$$\int_{x_1}^{x_2} F\,dx = \int_{\varphi_1}^{\varphi_2} Ni\,d\varphi - (U_2 - U_1). \tag{6}$$

The first right-hand term is represented in Fig. 2 by the area 5–1–2–6 while U_1 and U_2 are represented respectively by the areas 0–1–5 and

0–3–2–6. Thus the mechanical work, the left-hand term of equation (6), is represented by 0–1–2–3–0, the area bounded by the two magnetization curves and the path followed by φ, x and Ni in the concurrent change from I_1 at x_1 to I_2 at x_2.

If armature motion occurs at constant flux, the first right-hand term in equation (6) is zero, and the mechanical work equals the change in the field energy U. If $\varphi = \varphi_3$ in Fig. 2 for example, the work done as the armature moves from x_1 to x_2 is $U_4 - U_3$, represented by the area 0–4–3–0. From equation (6), the pull F is then given by:

$$F = -\frac{\partial U}{\partial x} \quad (\varphi \text{ constant}). \tag{7}$$

If armature motion occurs at constant current, the first right-hand term in equation (6) becomes the change in $NI\varphi$. If $I = I_1$, for example, motion of the armature from x_1 to x_2 increases $NI\varphi$ from $NI_1\varphi_1$ to $NI_1\varphi_3$. Hence the mechanical work done is the difference between $NI_1\varphi_1 - U_3$, represented by the area 0–3–8 and $NI_1\varphi_1 - U_1$, represented by the area 0–1–8. The work done at constant current is therefore the change in the quantity W defined by the equation:

$$W = \int_0^{NI} \varphi \, d(NI),$$

which is represented by the area between the magnetization curve and the NI axis. From equation (6), the pull F is given by:

$$F = \frac{\partial W}{\partial x} \quad (I \text{ constant}). \tag{8}$$

The pull F can therefore be determined either from equation (7) or from equation (8), provided the magnetization curves are known. These equations may be applied graphically or numerically to compute the pull in specific cases. They may also be used, as shown in Section 7, to obtain expressions for the pull from expressions for the magnetization relations. In addition, they afford the following graphical interpretation of the dependence of the mechanical output upon the magnetization relations, the current, and the armature travel.

If x_1 in Fig. 2 represents the unoperated position of the armature, and x_2 its operated position, the work that can be done at constant current is $W_2 - W_1$, which varies with the value of I applying. For small values of I, for which both magnetization curves are linear, the work capacity $W_2 - W_1$ varies approximately as $(NI)^2$. At higher values of NI, the two magnetization curves approach each other as they approach the

limiting saturation flux, and the rate of increase of $W_2 - W_1$ becomes progressively smaller. The saturation flux therefore puts a ceiling on the mechanical work attainable.

If the armature travel is increased, increasing the unoperated gap x_1, the corresponding magnetization curve is lowered, reducing W_1 with a consequent increase in the work capacity. However large x_1 may be made, there remains a leakage field, to which corresponds a limiting magnetization curve. An extreme upper limit to the work capacity is represented by the area between this limiting magnetization curve and that for the operated position of the armature.

The magnetization curves thus suffice for the evaluation of both the field energy and the mechanical output associated with armature motion, and therefore completely define the static performance of the electromagnet. The problem of relating this performance to the design then reduces to the problem of relating the magnetization characteristics to the design.

3 THE MAGNETIC CIRCUIT CONCEPT

A rigorous determination of the magnetization relations from the dimensions and configuration of the electromagnet would require the solution of the static magnetic field equations. For the geometry obtaining in actual structures, such solutions can at best be obtained only for specific cases, and then only by tedious numerical or graphical methods. Approximate solutions, however, may be obtained by a procedure in which the actual distributed field is taken as confined to a limited number of paths, which together form a network analogous to an electrical circuit. The extent to which this procedure may provide a valid approximation is indicated in the following brief review of the basic postulates of static field theory. For the present purpose, these may be stated as follows:

The energy of a static magnetic field is the volume integral of the product of the magnitudes of the B and H vectors over the space containing the field. These vectors coincide in direction at all points, and are subject to the conditions: (1) that B can be represented by closed continuous lines, ("lines of induction"), whose density measures the magnitude of B, (2) that the ratio μ of B to H at any point is determined by the medium in which the point is located, (3) that the line integral of H around a closed path is equal to 4π times the total current in all circuits linking this path. This integral is the magnetomotive force $\mathfrak{F}$; it has the value $4\pi NI$ for a coil of N turns with current I flowing in them.

For a rigorous general treatment, these postulates must be expressed in differential form (the field equations), and solutions obtained in which they are satisfied at all points within the field. They may be applied directly, however, in certain cases of simple symmetry, and this same treatment, to some measure of approximation, may be used more generally. To do this, the lines of induction measuring B can be considered as grouped into tubes of induction. Each such tube is, from the properties of B, continuous, and the integral of B over a cross section of the tube is a constant quantity φ, characterizing this tube. Over a length of tube $\Delta\ell$ bounded at its ends by two surfaces over each of which H is constant exists a difference in magnetic potential, $\Delta\mathfrak{F}$, equal to the line integral $\int H d\ell$. Then $\Delta\mathfrak{F} = \varphi\Delta\mathfrak{R}$ where $\Delta\mathfrak{R}$ is the reluctance of this portion of the tube, determined by its dimensions and the permeability μ of the medium. In particular, for a tube of uniform cross-section a over length ℓ, $\Delta\mathfrak{R} = \ell/(\mu a)$. More generally, if two equipotential surfaces can be identified, bounding a region of constant permeability (such as an air gap), the solution of Laplace's equation for the region bounded by these surfaces permits the evaluation of the flux between them, and thus of the reluctance $\Delta\mathfrak{R}$.

It follows that if the pattern of the field can be recognized, so that the boundaries of some major tube of force can be determined, the reluctance of its several sections can be evaluated, and their sum $\Sigma\Delta\mathfrak{R}$ or $\mathfrak{R}$, is the ratio $\mathfrak{F}/\varphi$, where φ is the flux of the tube and $\mathfrak{F}$ the magnetomotive force of the coil linking it.

The possibility of recognizing the approximate pattern of the field results from the high values of the permeability of magnetic materials to that for air, μ_a. The ratio μ/μ_a is in excess of 1000 under normal conditions of operation. Hence the reluctances of air paths are large compared with those through magnetic material, the tubes of induction tend to follow a path through the iron, and the major changes in magnetic potential occur where they pass through air gaps. In an electromagnet such as that of Fig. 3(a), the major tube of induction follows a path through the core and armature, and the potential drops balancing the applied magnetomotive force $\mathfrak{F}$ appear principally at the air gap separating surface 1 from surface 2, and at the heel gap separating surfaces 3 and 4. There will be little potential difference between 4 and 5, but the large potential difference between this region and surface 1 will result in a leakage field between them.

Thus the total flux φ linking the coil can be considered as divided into tubes of induction φ_A and φ_{LC} following the paths indicated in Fig. 3(a).

φ_A can be considered as subdivided in turn into φ_{LA} and φ_G representing respectively a leakage field from 2 to 1, and a field concentrated at the air gap between these surfaces.

These tubes of induction are analogous to the currents in an electrical network, and the applied magnetomotive force is analogous to the applied voltage producing these currents. The reluctances between equipotential surfaces are analogous to the resistances of the electrical network, and the potential differences between these surfaces are analogous to the voltage drops in the electrical resistances.

The field relationships involved may therefore be represented as in Fig. 3(b), in which the diagram of a resistance network indicates how the component reluctances determine the relation between the applied magnetomotive force $\mathfrak{F}$ and the resultant flux φ. The potential difference between the points 1 and 5 at the ends of the coil is $\mathfrak{F}$ less $\varphi\mathcal{R}_C$ where $\mathcal{R}_C$ is the reluctance of the core. This net potential balances the drop $\varphi_{LC}\,\mathcal{R}_{LC}$ across the leakage path and the drop through the armature path,

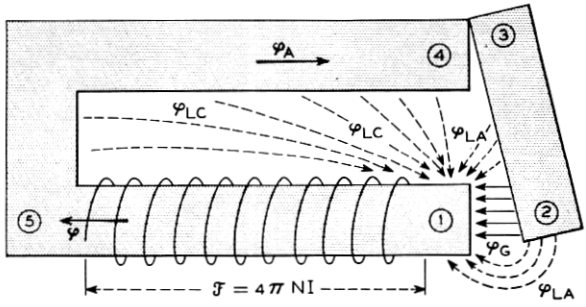

(a) MAGNETIC FIELD SCHEMATIC

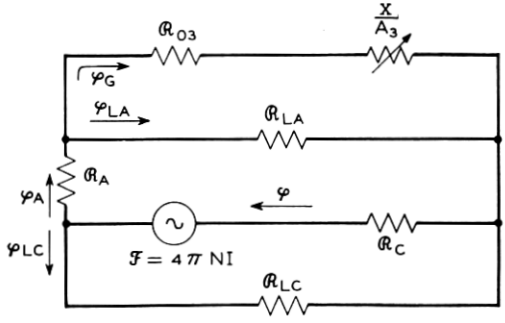

(b) MAGNETIC CIRCUIT

Fig. 3 — Magnetic circuit representation of magnetic field relations.

comprising the drop $\varphi_A \mathcal{R}_A$ through the iron part of this path in series with that across the two parallel paths followed by φ_{LA} and φ_G.

Obviously, this pattern can be elaborated and made more exact by more detailed consideration, particularly with respect to the leakage field across the coil, which is not wholly confined to that between its ends. In general, the field may be divided to any desired degree of refinement into tubes of induction, which may then be treated as a network. Thus, in principle, magnetic circuit representation may be used to evaluate the magnetization relations to any desired degree of accuracy.

Determination of the magnetization relations is thus reduced to the evaluation of the reluctances appearing in the magnetic circuit. These include both the reluctances of the iron parts for the major tubes of induction directed along the axes of these parts, and the reluctances of the air gaps and leakage paths. To evaluate these reluctances there are needed (1) values of the permeability of magnetic materials, as related to the flux density within them, and (2) expressions for the reluctances of gaps and leakage paths. These two topics are discussed in the sections following. While much of the material in these two sections is familiar, it is reviewed here with emphasis on the analytical formulation of the relations involved.

4 MAGNETIZATION CHARACTERISTICS OF MATERIALS

Magnetic properties are expressed either in terms of the relation between the permeability μ and the induction B, or of that between B and the potential gradient H, from which the $\mu - B$ relation is derived. The experimental determination of this relation is most commonly made with a uniformly wound ring sample, in which B and H are uniform throughout.

For increasing magnetization, as in relay operation, the pertinent $B - H$ relation is that obtained with an initially demagnetized specimen, shown as the solid line in the first quadrant in Fig. 4. This is the normal magnetization curve. It is nearly coincident with the locus of the terminal points (such as 1 and 2) of hysteresis loops obtained by cyclic magnetization and demagnetization.

The normal magnetization curve for magnetic iron is shown in Fig. 5 together with the corresponding $\mu - B$ curve. The permeability increases from its initial value μ_0 to a maximum value μ' at a density B' corresponding to the "knee" of the $B - H$ curve. (The single prime superscript is used throughout this paper to designate values of the various magnetic constants at maximum permeability.) Thereafter μ declines,

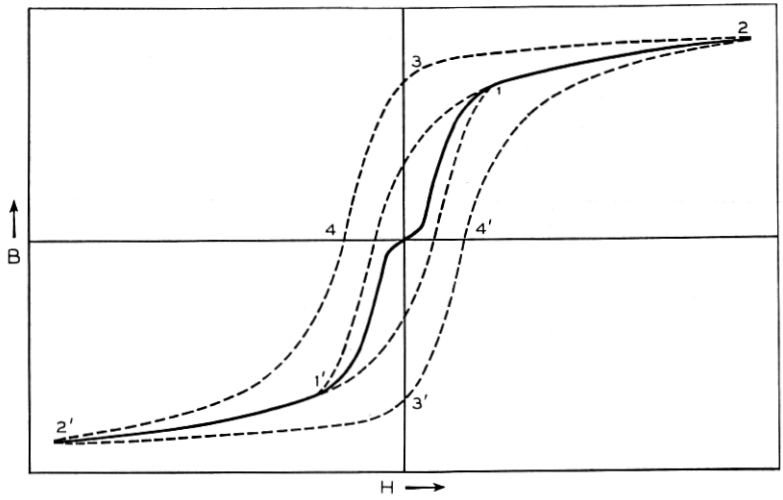

Fig. 4 — Cyclic magnetization relations.

and can be considered to approach zero as B approaches the saturation density B''.

In the design and operation of ordinary electromagnets, the aspects of the $\mu - B$ relation of practical importance are (1) the order of magnitude of μ through the central portion of the curve, which determines the approximate magnitude of the (minor) contribution of the iron path to the total reluctance, and (2) the value of B at which μ becomes relatively small (less, for example, than 1000). At or near this value of B, the magnetic path reluctance increases rapidly for small increments in B, limiting the field strength and pull attainable. In the core, this limiting value of B, together with the cross section a, limits the flux $\varphi(=aB)$ which the core can supply; conversely, this value of B establishes the core cross-section a required to attain a desired value of φ. The exact value of B which is effectively limiting varies with the design conditions, but is approximately measured by the density B_M at which μ equals 1000.

Demagnetization Relations

For decreasing magnetization, as in relay release, the pertinent $B-H$ relation is the return portion of the major hysteresis loop, the loop starting from a point on the normal curve near saturation, such as the loop 2–3–4 of Fig. 4. Nearly the same loop is obtained for any location of the point 2 well beyond the knee of the curve. The distinguishing feature of this relation is the existence of the remanence B_R at the point 3, where

$H = 0$. To account for this there must be added to the magnetic postulates cited above the assumption that there may be a movement of electric charge within the material which supplies an effective mmf per unit length measured by the coercive force H_c, represented in Fig. 4 by the distance from the origin to the point 4.

When the coil circuit is opened in relay release, the coercive force of the core material results in a residual flux passing through the air gaps in series with the iron path. A potential drop $\mathfrak{F}$ must exist across these gaps. In the absence of applied magnetomotive force, this must be balanced by an equal and opposite drop through the core. There is thus an imposed negative potential gradient $-H$ per unit length of the core. The remanence B_R is therefore governed by the $B-H$ relation in the second quadrant, the curve 3–4 of Fig. 4. This is the demagnetization relation, as illustrated separately in Fig. 6. The intercepts of this curve on the B and H axes are H_c and B_R.

If $\mathfrak{R}_E$ is the reluctance of the magnetic circuit external to the core, the external drop $\mathfrak{F}_E$ equals $\mathfrak{R}_E\varphi$, where φ is the flux. Taking B and H as uniform in the core, $\varphi = Ba$ and $\mathfrak{F}$ equals $H\ell$, where a and ℓ are the cross-sectional area and length of the core. The values of B and H in the core must therefore conform to the equation:

$$-\frac{B}{H} = \frac{\ell}{a\mathfrak{R}_E}. \tag{9}$$

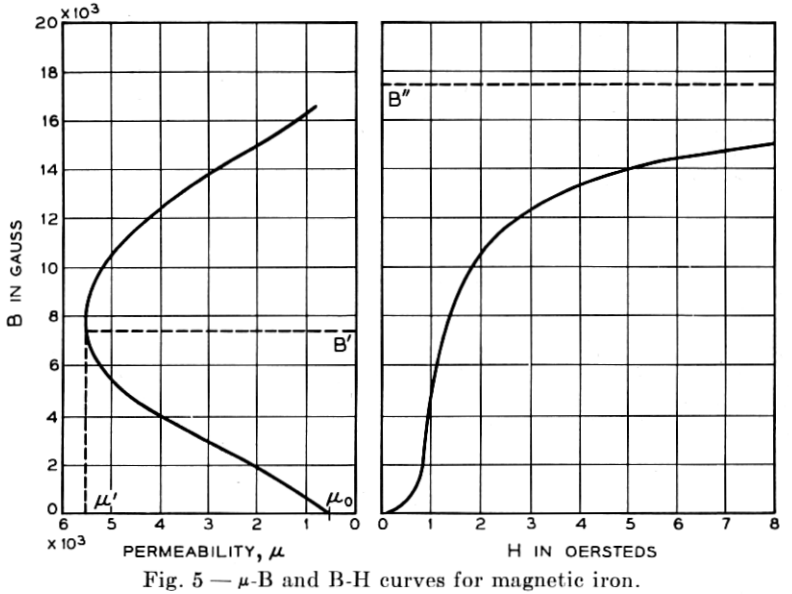

Fig. 5 — μ-B and B-H curves for magnetic iron.

As illustrated in Fig. 6, B and H are therefore determined by the intersection with the demagnetization curve of the line having a slope given by the right-hand side of (9). The complete magnetic circuit has a residual flux $\varphi = Ba$ resulting from the coercive mmf, $H_c\ell$, which equals the sum of the potential drop $H\ell(=\Re\varphi)$ external to the core and the drop $(H_c - H)\ell$ in the core.

Properties of Magnetic Materials

The properties of the magnetic materials commonly used for electromagnets are shown in Table I. This includes, in addition to the magnetic properties, the working properties in manufacture, and the resistivity. The latter determines the eddy current delay in otherwise similar structures, and is a controlling factor where fast release is desired.

For design purposes, allowance must be made for variations in the material, which are relatively large in the case of magnetic properties. Minimum and maximum values are therefore given in Table I. As indicated by the footnote in this table, H_c is subject not only to initial variation, but to an increase with time: "aging." The relatively large magnitude of this change for magnetic iron is a serious disadvantage in

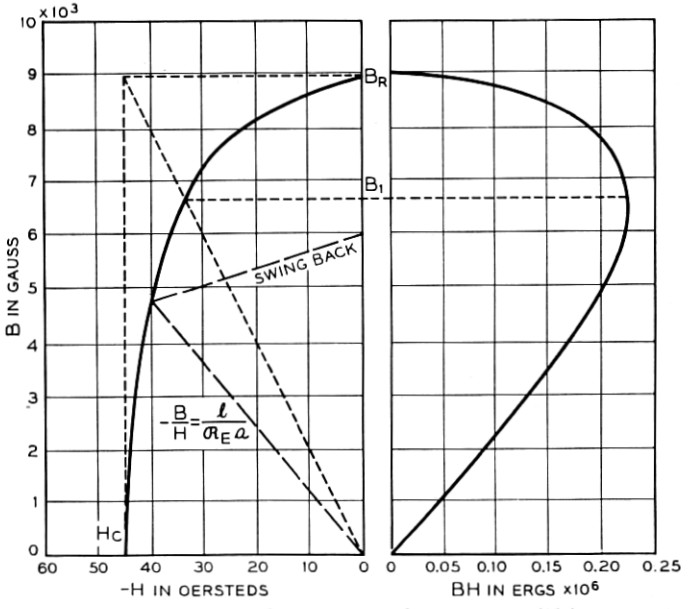

Fig. 6 — Demagnetization and energy product curves (1½ per cent chrome steel).

TABLE I — SOFT MAGNETIC MATERIALS

Material	Magnetization				Demagnetization				Resistivity Microhms cm^{-1}
	μ_{max}		B_M† (gauss)		B_R (gauss)		H_C (oersteds)		
	Min.	Max.	Min.	Max.	Min.	Max.	Min.	Max.	
Magnetic iron									
Sheet	4,300*	12,000	15,500	16,200	10,500	15,000	0.5	1.4*	11
Rod	4,300*	8,000	15,500	16,200	10,500	12,000	0.5	1.4*	11
Mild steel	2,200	7,500	14,000	16,000	7,800	15,000	0.8	2.5	12
Cast iron	(Nominal: 600)		(B″ = 10,000)		—	—	—	—	25
1% silicon iron	4,000	15,000	14,700	15,600	9,000	14,500	0.4	1.4	25
2½% silicon iron	4,000	12,000	14,000	15,000	8,000	12,000	0.4	1.4	40
4% silicon iron	5,000	12,000	13,500	15,000	8,000	12,000	0.3	1.1	60
H_2 anneal iron									
Sheet	7,000	15,000	15,500	16,500	14,000	15,000	0.5	0.9	11
Rod	4,500	8,000	15,500	16,500	12,000	14,000	0.7	1.0	11
45 permalloy	15,000	60,000	14,000	15,000	8,000	12,000	0.1	0.4	50
78 permalloy	50,000	250,000	10,000	10,400	5,000	7,500	0.02	0.1	16
Nickel	(Nominal: 600)		(B″ = 6,000)		—	—	—	—	8

* After aging, μ_{max} for magnetic iron may be as low as 3000, and H_C as high as 2.5.

† B_M: Density for $\mu = 1000$. B″: Saturation density.

applications in which release performance is important. Aging also reduces the permeability. In materials other than magnetic iron, the aging effect is relatively minor.

Because it is cheap and easily fabricated, magnetic iron has been the most commonly used magnetic material in Bell System relays and switching electromagnets. Other materials, particularly 45 permalloy, have been used in special applications where the improvement in performance, as in higher sensitivity or faster release, warranted the increased cost. The superiority of the permalloys in these respects is offset for heavy duty applications by the lower level of flux attainable with a given core cross-section, as measured by B_M.

The silicon steels are comparable with magnetic iron in cost, and similar in magnetic properties, except for slightly smaller values of B_M. They are, however, superior in their relative freedom from aging, and in their higher resistivity. These advantages are offset, in the case of the 4 per cent material, by its hardness and brittleness. All the silicon steels are used in sheet form for the construction of transformers and electrical machines. The 1 per cent and 2½ per cent materials are available in rod and bar form, and have working properties intermediate between those of magnetic iron and 4 per cent silicon iron. Because of its advantages in aging and resistivity, 1 per cent silicon iron has been used in preference

to magnetic iron in the recently developed wire spring general purpose relay.

Magnetic iron is a very low carbon steel of high purity. Commercial mild steel, properly annealed, will serve as an adequate substitute where the spread in properties shown in Table I can be tolerated.

In magnet design, casting offers the possibility of providing a more complex one-piece configuration than can be obtained with punched and formed parts. Casting is rarely used in current magnet construction — an illustrative exception is the British Post Office stepping magnet for their step-by-step switch. Grey cast iron has been a preferred material for this type of construction.

The properties of nickel are included because of its use as a magnetic separator and hinge member.

Hyperbolic Approximation to Magnetization Curves

The variation of permeability with density makes it necessary to provide some formulation of the μ versus B relation in developing an analytical treatment of magnetization relations. The B versus H relation for decreasing magnetization, the loop 2–3–4 of Fig. 4, has a shape similar to that of a rectangular hyperbola, asymptotic to the line representing B''. This curve can therefore be represented approximately by the equation:

$$\frac{B}{B'' - B} = \frac{\mu''}{B''}(H_c - H), \tag{10}$$

in which μ'', B'', and H_c are constants.

This purely empirical relation is called the Froelich-Kennelly equation. In general, it does not give a satisfactory fit to the whole loop, but provides a satisfactory approximation for engineering use to the portions of the curve in either the first or second quadrants, using different values for the constants in the two cases. In addition, it may be employed to represent the upper portion of the normal, or increasing magnetization curve.

The expression for the permeability μ, or $B/(H_c + H)$ corresponding to (10) is:

$$\frac{1}{\mu} = \frac{1}{\mu''} + \frac{H_c + H}{B''}. \tag{11}$$

Hence, to the extent the B—H curve conforms to equation (10), the reciprocal of the permeability varies linearly with H. Alternately, the

permeability may be expressed in terms of B, giving the equation:

$$\mu = \frac{\mu''(B'' - B)}{B''} . \tag{12}$$

If this relation is applied to a part of a magnetic circuit, such as the core of a relay, the reluctance $\mathcal{R}_C$ of this part may be written as $\ell/(\mu a)$, where ℓ is the length and a is the cross-sectional area of the part. Then from (10), $\mathcal{R}_C$ is given by:

$$\mathcal{R}_C = \mathcal{R}_C'' \frac{\varphi''}{\varphi'' - \varphi} , \tag{13}$$

where $\mathcal{R}_C'' = \ell/(\mu'' a)$, $\varphi = Ba$, the flux through the part, and φ'' is the saturation value of φ.

For increasing magnetization, this expression is applicable only for values of B, or φ/a, beyond the knee of the magnetization curve, the point of maximum permeability. Thus (13) is applicable for values of B above B', the density at which μ has its maximum value μ'. Writing $\mathcal{R}_C'$ for $\ell/(\mu' a)$ and φ' for $B'a$, (13) may be written in the alternative form:

$$\mathcal{R}_C = \mathcal{R}_C' \frac{\varphi'' - \varphi'}{\varphi'' - \varphi} . \tag{13A}$$

For values of B below B' the permeability of initially demagnetized material varies greatly with B, as shown in Fig. 5. In normal use, however, an electromagnet is rarely operated from a fully demagnetized state. Fig. 7(a) shows the magnetization relations for an electromagnet in repeated operation, and Fig. 7(b) shows the corresponding relations for its core. The solid line corresponds to initial operation from a demagnetized condition, the dotted line to decreasing magnetization in release, and the dashed line to subsequent remagnetization. The latter corresponds to higher permeability and a lower core reluctance than those for initial magnetization. As a convenient approximation, linear magnetization may be taken as a representative condition for B less than B', in which case the core reluctance is constant for φ less than φ'. In this low density region, then, the magnetic circuit constants may be considered to be independent of the flux. This, of course, is never strictly true, but it is a satisfactory approximation for most ordinary electromagnets.

Hyperbolic Approximation to Decreasing Magnetization Curves

As the hyperbolic approximation is a purely empirical relation, it may be applied to the $\varphi - \mathfrak{F}$ relation for an electromagnet as well as to that

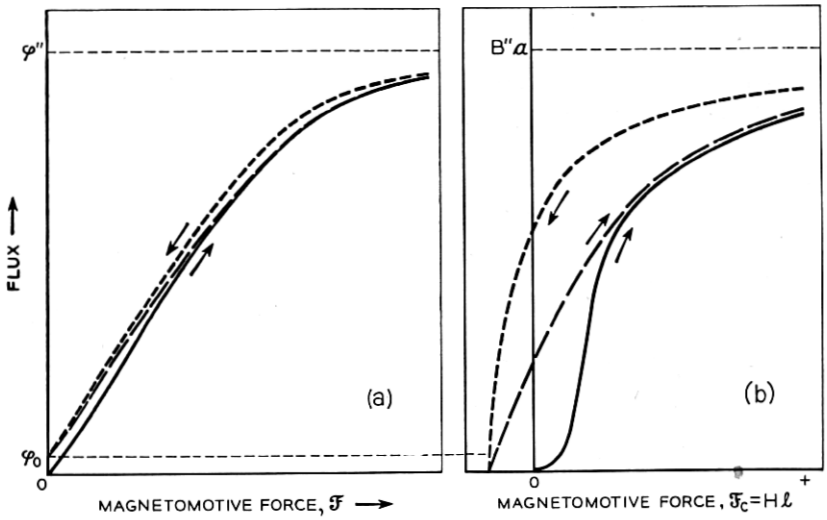

Fig. 7 — Repeated magnetization of an electromagnet and its core.

of a core or other part. It is convenient to use it in this way for the decreasing magnetization relation, as this is of interest only for a single value of the gap reluctance, that for the operated position.

The decreasing magnetization relations for an electromagnet and for its core are shown in Figs. 7(a) and 7(b) respectively. For decreasing magnetization, a residual flux φ_o remains when $\mathcal{F}$ is reduced to zero, determined by the same equilibrium conditions as apply to permanent magnets. The curve for the magnet, Fig. 7(a), must pass through φ_o and be asymptotic to the saturation flux φ''.

This relation between φ and $\mathcal{F}$ may be represented by an equation of the same form as equation (10), with B and B'' replaced by φ and φ'', with H and H_C replaced by $\mathcal{F}$ and $\mathcal{F}_C$, and the constant μ'' replaced by $1/\mathcal{R}''$. Using the condition that $\varphi = \varphi_o$ for $\mathcal{F} = 0$ to eliminate $\mathcal{F}_C$, the equation may be written in the form

$$\frac{\mathcal{F}}{\mathcal{R}''\varphi''} = \frac{\varphi}{\varphi'' - \varphi_o} - \frac{\varphi_o}{\varphi'' - \varphi_o}. \tag{14}$$

If the length ℓ and cross-section a of the core are known, together with the magnetic constants of the core material and the reluctance $\mathcal{R}$ of the return path (external to the core), the constant terms in (14) may be evaluted. φ'' is equal to aB'', where B'' is the saturation density of the core material. As previously noted, the values of B_M in Table I may be used as effective values of B''. φ_o may be evaluated as the permanent

magnet flux supplied by the core to an external path of reluctance $\mathcal{R}$, using equation (9) and the demagnetization curve for the core material. $\mathcal{R}''$ may be determined from the initial slope $\mathcal{R}_i = d\mathcal{F}/d\varphi$ at $\mathcal{F} = 0$. By differentiation of equation (14), this initial slope is given by the equation:

$$\mathcal{R}_i = \left(\frac{\varphi''}{\varphi'' - \varphi_o}\right)^2 \mathcal{R}''. \tag{15}$$

$\mathcal{R}_i$ may be evaluated as the sum of the core reluctance and the external reluctance $\mathcal{R}$. In determining the core reluctance, μ should be taken as the incremental permeability, or the slope of the demagnetization curve at $B = \varphi_o/a$. With $\mathcal{R}_i$ thus evaluated, $\mathcal{R}''$ is given by equation (15).

5 MAGNETIC RELUCTANCES AND CONDUCTANCES

As shown in Section 3, determination of the magnetization or $\varphi - \mathcal{F}$ relations is equivalent to determining the reluctance $\mathcal{R}$, or $\mathcal{F}/\varphi$, and this in turn reduces to the determination of the component reluctances of the magnetic circuit. Some of the more useful expressions for the evaluation of these component reluctances are given in this section. Where parallel paths appear, the computations involve the reciprocals of reluctances. It is convenient to refer to the reciprocal of a reluctance as a magnetic conductance, or permeance.

Toroid

The magnetic field of a toroidal coil is shown in Fig. 8. Provided the medium within the coil is homogeneous, and the section diameter small compared with the toroid's diameter, symmetry requires the field to have the simple character shown. As $\mathcal{F} = H\ell$ and $B = \mu H$,

$$\mathcal{R} = \frac{\mathcal{F}}{\varphi} = \frac{H\ell}{\mu H a} = \frac{\ell}{\mu a}, \tag{17}$$

which applies whether the path is in iron or air.

If the toroid is of iron, and the coil is concentrated over part of the length, some of the field appears outside the toroid. This effect is secondary, and (17) still applies to a close approximation. If a cut is made and an air gap introduced, the total reluctance is greatly increased, but the field within the toroid retains the same character except near the gap. The reluctance of the iron path, now in series with the air gap reluctance, is given by (17). This expression is therefore of general use in determining the reluctance of iron parts of length ℓ and uniform cross-section a.

Air Gap Between Parallel Planes

For magnetic paths in which the flux is uniform, it was shown above that the reluctance is given by (17). This applies to the case of an air gap between parallel planes of area A, as shown in Fig. 9, where the length of the path is the separation x. The reluctance of such a gap may therefore be written as:

$$\mathcal{R} = \frac{x}{A}.$$

In this, as in subsequent expressions for air gap reluctance, the multiplier $1/\mu_a$, which is the reciprocal of the permeability of air, is omitted for convenience. In CGS units, $\mu_a = 1$.

Special Gap Shapes

The simple relation just given provides a basis for the calculation of more complex shapes. For example, the reluctance of the wedge shaped gap of Fig. 10 may be found by assuming tubes of flux in parallel throughout the gap. Then the permeance of an elementary path is $\Delta\mathcal{P} = b\Delta r/r\theta$ and the total permeance of the gap is the sum of these elementary paths, or:

$$\mathcal{P} = \frac{b}{\theta}\int_{r_1}^{r_2}\frac{dr}{r} = \frac{b}{\theta}\ln\frac{r_2}{r_1}.$$

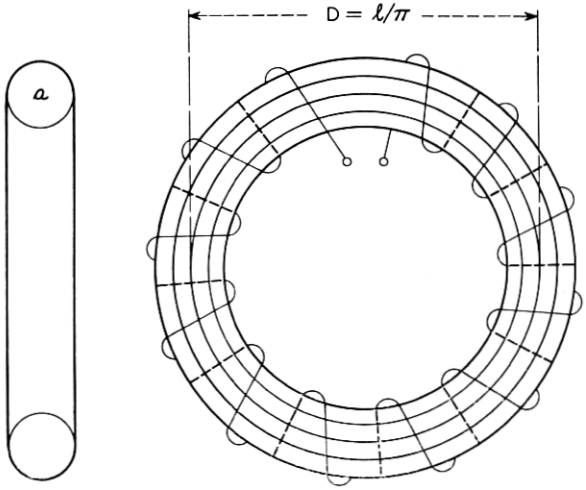

Fig. 8 — Field of a uniformly wound toroidal core.

The reluctance, as given in the figure, is the reciprocal of this.

For the gap of Fig. 11, it is more convenient to estimate reluctances, summing the elementary series contributions to the entire gap. For this case:

$$\Delta\mathcal{R} = \frac{\Delta r}{br\theta},$$

where

$$\mathcal{R} = \frac{1}{b\theta}\int_{r_1}^{r_2}\frac{dr}{r} = \frac{1}{b\theta}\ln\frac{r_2}{r_1},$$

as noted in the figure.

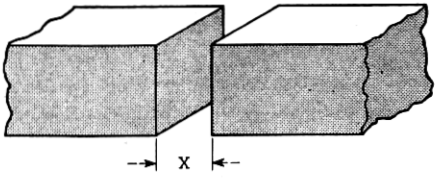

$\mathcal{R} = \frac{X}{A}$

WHERE A = AREA OF ONE POLE FACE

IF THE TWO POLE FACE AREAS ARE UNEQUAL, USE THE SMALLER VALUE

Fig. 9 — Reluctance between parallel plane surfaces.

Effective Pole Face Area of an Electromagnet

As illustrated in Figs. 9, 10, and 11, an individual air gap has a reluctance represented approximately by an expression of the form:

$$\mathcal{R} = \frac{x}{A},$$

where x is the separation measured at the centroid of the area A. Armature motion is usually rotary, and a convenient point for the measurement of armature position may be at some distance from the axis other than that of the centroid. If x is so measured, then the separation at the centroid is kx, where k is the ratio of the lever arms, and hence the reluctance $\mathcal{R}$ is kx/A, equivalent to that of a gap of separation x and pole face area A/k. This area A/k is called the effective pole face area referred to the point at which x is measured.

In general, an armature has at least two gaps, as illustrated in Fig. 12. The expression for the armature reluctance must include the terms for both gaps which can conveniently be combined as follows. Let x be the armature motion measured at some distance ℓ from the axis of rotation, as indicated in the figure. Let k_1x be the corresponding separation at the centroid of a_1, and k_2x the separation at the centroid of a_2. Then the

reluctance of the combination is:

$$\mathfrak{R} = x\left(\frac{k_1}{a_1} + \frac{k_2}{a_2}\right).$$

It follows that the reluctance of the combined gap is equivalent to that of a simple gap with an effective pole face area given by:

$$\frac{1}{A} = \frac{k_1}{a_1} + \frac{k_2}{a_2}. \tag{18}$$

Exact: $\mathfrak{R} = \dfrac{\theta}{bln\left(\dfrac{1 + \dfrac{a}{2r_0}}{1 - \dfrac{a}{2r_0}}\right)}$

Approximate: $\mathfrak{R} = \dfrac{x}{ab}$

Errors of approximation:

Less than 1 per cent if $a < \frac{1}{3}r_0$

and/or $x < \frac{1}{2}r_0$

Less than 10 per cent if $a < r_0$

and/or $x < \frac{4}{3}r_0$

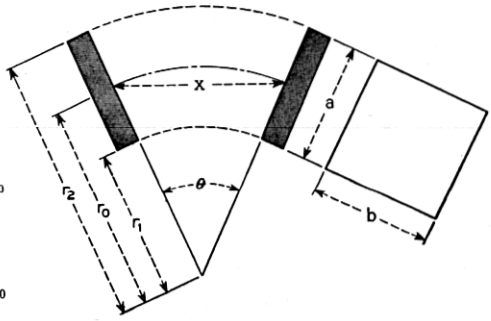

Fig. 10 — Reluctance between inclined plane surfaces.

Exact: $\mathfrak{R} = \dfrac{ln\,\frac{r_2}{r_1}}{b\theta}$

Where b = length parallel to axis

Approximate: $\mathfrak{R} = \dfrac{x}{br_0\theta}$

Errors of approximation:

Less than 1 per cent if $r_2 < 1.4r_1$,

Less than 10 per cent if $r_2 < 3r_1$,

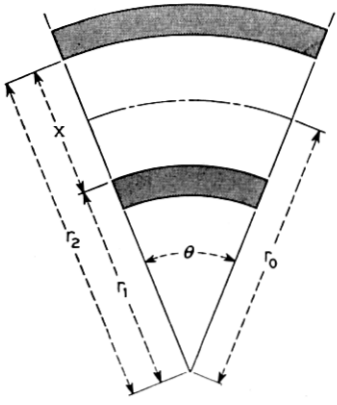

Fig. 11 — Reluctance of a cylindrical gap.

Leakage Reluctances

An accurate estimate of the reluctance between magnetic members requires a detailed knowledge of the flux paths. Since these are only known accurately in cases for which solutions of the field equations are available, approximations are obtained by assuming geometrical paths such as straight lines, arcs of circles, ellipses, and so forth. From these assumed paths the reluctance is calculated by means of the expression $\ell/\mu a$. The choice of suitable approximations depends largely upon a knowledge of the flux paths in certain simple cases which can be analyzed rigorously, and upon the experimental exploration of more complicated fields.

The method is satisfactory provided the separation between the magnetic members is small. It has been used to derive the relations given in Figs. 10 and 11. A further application of this method gives the reluctance between the side surfaces of coaxial cylinders, as shown in Fig. 13. This is useful in estimating the leakage reluctance shunting an air gap.

Where the separation between magnetic members is large, it is difficult to estimate the configuration of the flux paths. It is then necessary to employ the relations applying to the most nearly similar configuration for which a rigorous solution is known. Two such solutions are applicable to a number of problems. The first is the case of two infinitely long, parallel, equipotential, circular cylinders, shown in Fig. 14. The second is the case of two equipotential spheres of equal size, shown in Fig. 15.

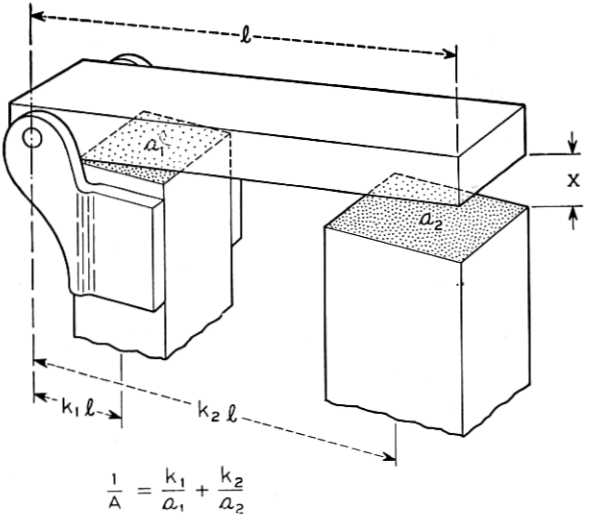

Fig. 12 — Effective pole face area referred to gap x at ℓ.

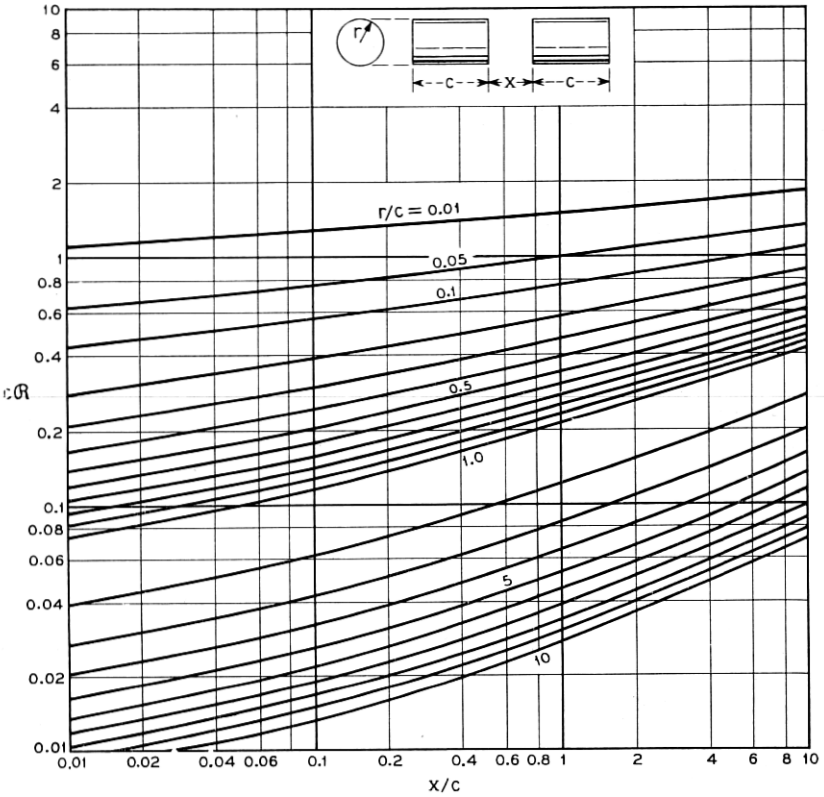

$$m = \ell n \left[1 + 2 \frac{c}{x} \left(1 + \sqrt{1 + \frac{x}{c}} \right) \right],$$

when $\frac{c}{rm} < 1$, $\qquad \mathfrak{R} = \dfrac{\cos^{-1}\left(\frac{c}{rm}\right)}{\pi rm \sqrt{1 - \left(\frac{c}{rm}\right)^2}}$,

when $\frac{c}{rm} = 1$, $\qquad \mathfrak{R} = \dfrac{1}{\pi c}$,

when $\frac{c}{rm} > 1$, $\qquad \mathfrak{R} = \dfrac{\ell n \left[\frac{c}{rm} + \sqrt{\left(\frac{c}{rm}\right)^2 - 1} \right]}{\pi rm \sqrt{\left(\frac{c}{rm}\right)^2 - 1}}$,

if cylinders are not circular, let $r = \frac{1}{2\pi} \times$ perimeter.

Fig. 13 — Reluctance between side surfaces of end-on coaxial cylinders.

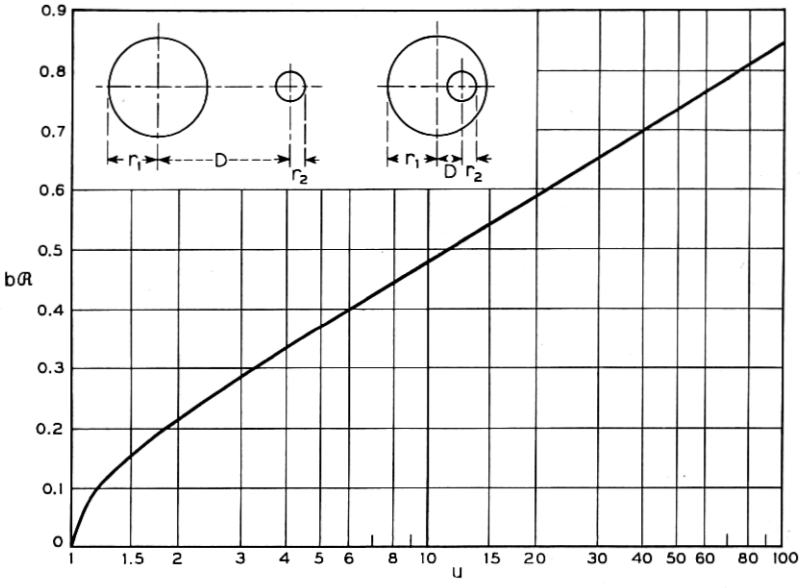

$$\Re = \frac{\ell n\left(u + \sqrt{u^2 - 1}\right)}{2\pi b} = \frac{COSH^{-1}u}{2\pi b}$$

where $u = \left| \dfrac{D^2 - r_1^2 - r_2^2}{2r_1 r_2} \right|$

and b = length of each cylinder

Fig. 14 — Reluctance between parallel cylinders.

For other configurations which bear a reasonable resemblance to the above cases, the leakage reluctances can be estimated satisfactorily by judicious modifications of the expressions for the simple cases.

For example, consider the case of two parallel rectangular bars. They are roughly equivalent to two parallel circular cylinders provided the minimum separation is the same in both cases, and provided the perimeter of each cylinder is equal to the perimeter of the corresponding bar. Thus, to estimate the leakage reluctance between the rectangular bars, the radius of each equivalent cylinder is taken as $1/2\pi$ times the perimeter of the corresponding bar, and the center-to-center distance between the equivalent cylinders is taken as the minimum separation between the two bars plus the two equivalent radii.

Leakage between the legs of many magnet forms may be estimated by

the approximation just described. Consider the idealized form shown in Fig. 16, where the magnetic path consists mainly of two parallel cylinders connected at one end, the armature and working gap being at the opposite end. The leakage flux in parallel with the main gap flux is determined by the reluctance of the path between these cylinders. For that portion of the two cylinders appearing outside the coil and therefore at approximately constant potential, the reluctance is found from the relations given in Fig. 14. For the leakage reluctance over the length enclosed by the coil, the drop in potential along the core results in one-third the previous reluctance, as is shown in Section 6. The variation in permeance per unit length for such cases may be found in Fig. 17.

Leakage also occurs between the end sections of many magnet forms, and may be estimated by a procedure similar to those above, assuming the end surfaces to be equivalent to two hemispheres having the same diameter d as the cylinders. The quantity $C_2 d$ in Fig. 17 is one half the permeance between corresponding spheres, as determined from the relations of Fig. 15. From this the net leakage permeance of leg and end

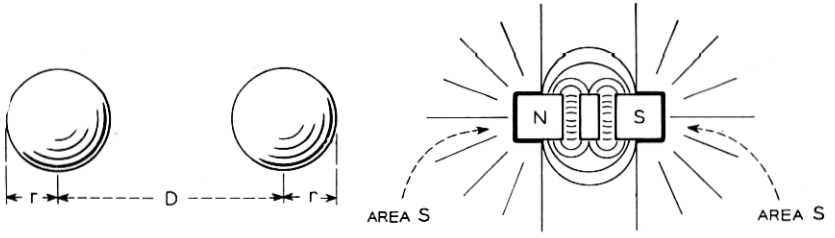

Exact: $$\mathfrak{R} = \frac{1}{2\pi r\left[1 + \left(\frac{r}{D}\right) + \left(\frac{r}{D}\right)^2 + \left(\frac{r}{D}\right)^3 + 2\left(\frac{r}{D}\right)^4 + 3\left(\frac{r}{D}\right)^5 + \ldots\right]}$$

Approximate: $$\mathfrak{R} = \frac{1 - \frac{r}{D}}{2\pi r}, \qquad \text{when } D > 6r$$

$$\mathfrak{R} = \frac{1}{2\pi r} = \frac{1}{\sqrt{\pi S}}, \qquad \text{when } D \gg r$$

where S = surface area of one sphere.

Latter approximation may be used to estimate leakage reluctance between back surfaces of pole pieces.

Fig. 15 — Reluctance between spherical surfaces.

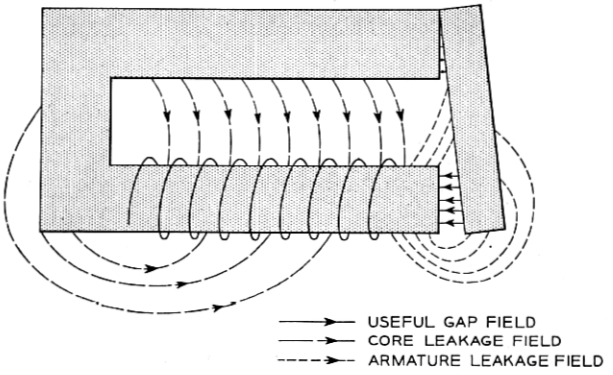

Fig. 16 — Distribution of the field of an electromagnet.

surfaces may be found as

$$\mathcal{P} = \frac{C_1 \ell_1}{3} + C_1 \ell_2 + C_2 d,$$

where values of C_1 and C_2 are given in curve form, and the equivalent value of d is as shown in Fig. 17. When the structure has two return paths, the reluctance is assumed to be one-half the value given by this last equation.

External Reluctance of a Bar Magnet

The relations of Figs. 13 through 17 suffice for the evaluation of leakage in most ordinary electromagnets. In special structures, particularly in polar relays, cases occur where the return path is predominantly an

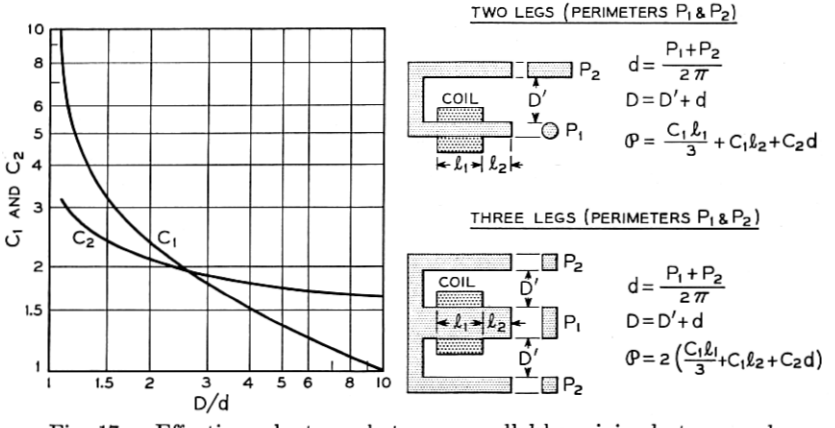

Fig. 17 — Effective reluctance between parallel bars joined at one end.

air path. A common case is that of a permanent magnet magnetized as a separate part prior to assembly in a polar structure. In such cases, the reluctance of the return path can be estimated as that of the external field of a bar magnet.

The reluctance of a bar magnet is closely represented by the reluctance of the same magnet in the form of a ring, in series with a reluctance representing all the flux return paths. Values for this reluctance may be assigned by measurements of magnetomotive force to produce a given flux in a ring sample and in a bar. The difference in magnetomotive force gives a measure of the reluctance of the air path. It has been found by

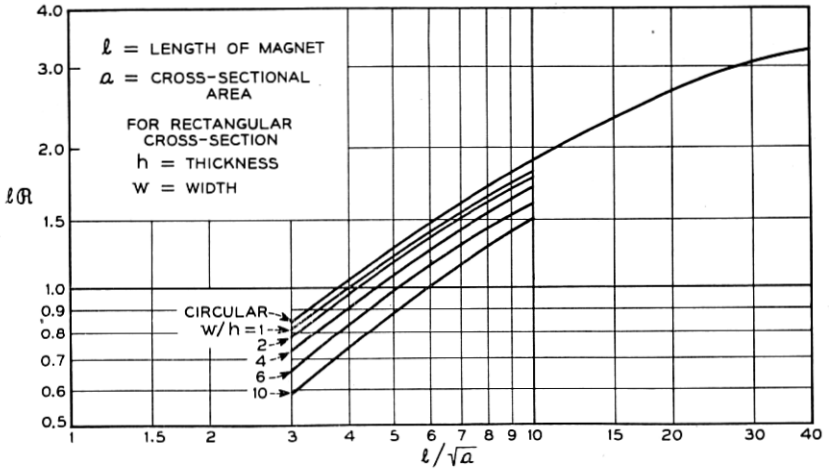

Fig. 18 — Effective leakage reluctance of a bar magnet.

Thompson and Moss[5] that the reluctance per unit length of bar depends on the shape of the bar cross-section, and is a function of the magnet dimensions $\ell/\sqrt{a}$, as indicated in Fig. 18. The reluctance so shown includes all flux lines emanating from the bar, and so may be thought of equally as leakage or effective reluctance.

Cases such as the bar magnet are difficult to estimate because of the variable flux density along the length of magnetic material. Calculations have been found possible only for the case of an ellipsoid, which is rarely met in practice.

Reluctance of a Solenoid

Another special case is that of the air field of a coil, which has the character shown in Fig. 19. This type of field obtains in the initial flux

decay of an electromagnet when the core is saturated. A similar condition applies to the leakage field of enclosed reed relays where the magnetic material constitutes only a small part of the inside cross-section of the coil. In such cases the reluctance of interest is that characterizing the complete magnetic circuit of an air core solenoid.

A number of simple relationships for various coil configurations follow from the identities between reluctance and inductance. Inductance is defined as the ratio of flux linkages to applied current:

$$L = \frac{N\varphi}{I} = \frac{4\pi N^2 \varphi}{4\pi N I},$$

from which:

$$\mathfrak{R} = \frac{\mathfrak{F}}{\varphi} = \frac{4\pi}{\left(\frac{L}{N^2}\right)}, \tag{19}$$

showing the inverse relationship between $\mathfrak{R}$ and the single-turn inductance L/N^2. Inductance for most of the usual coil configurations has been studied by Rosa and Grover[7] who give relations from which reluctance may be estimated. Most such expressions are quite involved; among the simpler is that for the case where b and c in Fig. 19 are small compared to a, given by:

$$\mathfrak{R} = \frac{0.2317a + 0.44b + 0.39c}{a^2},$$

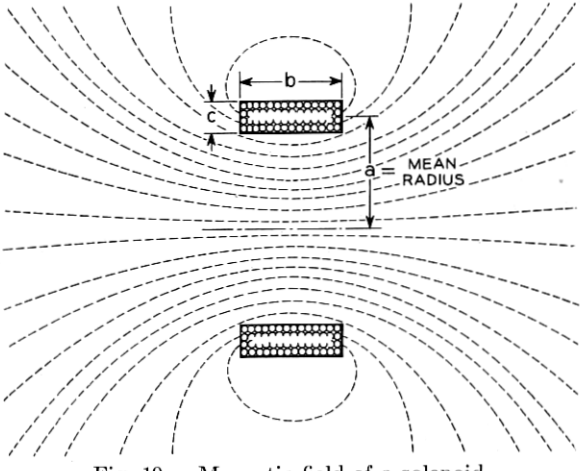

Fig. 19 — Magnetic field of a solenoid.

and Maxwell's approximation for coil of rectangular section:

$$\mathcal{R} = \frac{1}{a\left(\log \frac{8a}{R} - 2\right)},$$

where R = geometric mean distance of coil cross-section.

The examples described in the present section cover those procedures which are used most frequently in estimating leakage reluctances. For a more extended treatment of this subject, reference may be made to S. Evershed[3] and H. C. Roters.[4]

6 MAGNETIC CIRCUIT EVALUATION

In the discussion of the magnetic circuit concept in Section 3, it was noted that the accuracy of the representation varies with the extent to which the network of tubes of induction is sub-divided to correspond to the distributed nature of the actual field. The effect of sub-division upon the accuracy is greater in the high density region, where the reluctance of the iron parts is variable and increasing, than in the low density region, where the iron reluctance is small and approximately constant. Hence the choice of an adequate network is largely contingent upon the location of the iron parts having the highest flux density. Incipient saturation affects the reluctance of these parts, and thus the pattern of the field, while parts of lower density remain of low and approximately constant reluctance.

In ordinary electromagnets the core is the part of highest density, in which saturation limits the attainable field. It is good design practice to limit the core section to as small a value as is consistent with satisfactory performance, as this results in a minimum inside coil diameter. This is advantageous with respect to the coil constant, as shown by equation (1).

In the special case of high speed relays, it is advantageous to minimize the mass of the armature and hence its cross-section. In such relays armature saturation may control, or occur concurrently with core saturation. Saturation elsewhere than in the core or armature is of interest only in the diagnosis of faulty design, since the return members should have a section adequate to carry the maximum field at densities well below saturation.

Thus in most electromagnets, saturation occurs in the core, and incipient saturation affects its reluctance and the pattern of the associated field. The magnetomotive force varies along the length of the coil, and the core is therefore subject to variations along its length in magnetic

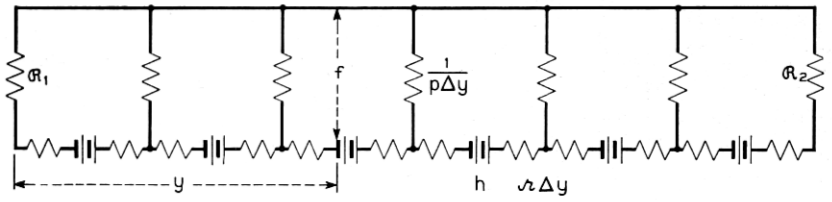

(a) TRANSMISSION LINE MAGNETIC CIRCUIT

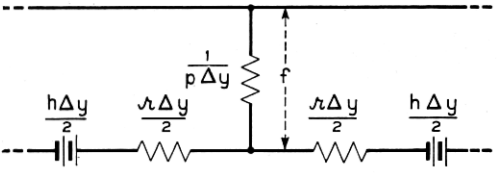

(b) DIFFERENTIAL LINE ELEMENT

Fig. 20 — Transmission line analogy to the field of an electromagnet.

potential, in flux density, and (at high densities) in reluctance per unit length. To treat it as a single circuit element, as in the discussion of Fig. 3, is thus a highly simplified approximation. An understanding of the extent to which this approximation is valid may be gained by considering a more rigorous analysis, in which, as indicated in Fig. 20, the core and return path are treated as analogous to a transmission line with distributed constants.

Transmission Line Analogy

In Fig. 20(a), the core is shown as one side of the line, and the return path as the other side. The length of the line is taken as the length of the winding, which is assumed to be distributed uniformly. It is assumed that the line is terminated at its ends by lumped reluctances, $\mathcal{R}_1$ and $\mathcal{R}_2$. The characteristics of the line and the applied magnetomotive force are expressed in terms of the following quantities:

f = mmf difference between the two sides of the line,
$\mathcal{r}$ = reluctance per unit length of line,
p = leakage permeance per unit length of line,
h = impressed mmf per unit length of line.

Instead of trying to represent the entire magnetic circuit by a simple network of a few lumped reluctances, it is assumed only that an infinitesimal length (dy) of the magnetic line can be represented by the "T"

network shown in Fig. 20(b). The complete magnetic circuit, then, consists of an infinite number of these elementary networks connected end-to-end and terminated in lumped reluctances at the extreme ends. Note that this approximation to the magnetic circuit explicitly recognizes the distributed nature of the leakage flux.

Consider now the several quantities which enter into the approximation. Each of the terminating reluctances ($\mathcal{R}_1$ and $\mathcal{R}_2$) includes two component reluctances in parallel. The first component is simply the leakage reluctance across the end of the line. The second component is the sum of the reluctances of the magnetic members and series air gaps which complete the circuit from one side of the line to the other. For any single value of the working gap, $\mathcal{R}_1$ and $\mathcal{R}_2$ may be taken as constants.

The quantity p, which is the leakage permeance per unit length between the two sides of the line, depends upon the geometry of the structure, and may be calculated by the methods of Section 5. Provided the configuration of the magnetic line is uniform throughout its length, p is taken as a constant. The assumption that p is constant is equivalent to assuming that all leakage paths between the two sides of the transmission line lie in planes that are perpendicular to the core. This condition is not satisfied near the ends of the core, but correction for the end effects may be made in evaluating the terminal reluctances, $\mathcal{R}_1$ and $\mathcal{R}_2$.

The quantity $\mathcal{r}$, the series reluctance per unit length of line, involves magnetic material whose permeability varies with flux density. It is a variable whose magnitude depends upon the applied magnetomotive force, upon the terminating reluctances, and upon position along the line, since it is a function of φ. In the low density region, however, its value is substantially independent of φ. Application of the magnetic circuit relations results in the following equations:

$$\frac{df}{dy} = h - \mathcal{r}\varphi, \tag{20A}$$

$$\frac{d\varphi}{dy} = -pf, \tag{20B}$$

whence:

$$\frac{d^2\varphi}{dy^2} = -p(h - \mathcal{r}\varphi). \tag{21}$$

Subject to the validity of the original assumptions, the solution of equation (21) describes the way in which the flux φ varies with y, the distance along the line.

At low densities, where $\mathcal{R}$ is constant, (21) may be solved to give a picture of the flux distribution in the magnet. The solution is obtained in terms of hyperbolic functions. The resulting expression is somewhat cumbersome, but reduces to a much simpler form in the special case where $\mathcal{R}$ is small compared with h. Neglecting $\mathcal{R}\varphi$, equation (20A) reduces to:

$$\frac{df}{dy} = h \qquad \text{or} \qquad f = hy$$

In this case then, the magnetomotive force varies linearly along the core, as was assumed in the discussion of Fig. 17 in Section 5.

For $f = hy$, equation (20B) becomes:

$$\frac{d\varphi}{dy} = -phy,$$

whence:

$$\varphi = \varphi_0 - \frac{phy^2}{2}, \tag{22}$$

where φ_0 is flux at $y = 0$ (one end), and ph is a constant for a given magnet structure. Thus, for this approximate case, the core flux falls off along its length approximately as the square of the distance from one end. The second term in (22) represents the leakage flux. For the whole core, for which $y = \ell$, the leakage flux is given by $p\,h\ell^2/2$, or by $p\,\ell\mathfrak{F}/2$. The average flux linked per turn, however, is the integral

$$\frac{1}{\ell}\int_0^{\ell} \frac{phy^2}{2}\,dy,$$

corresponding to a leakage reluctance of $p\ell/3$. Hence the factor 3 is used to evaluate the average flux linked per turn in Fig. 17.

From this consideration of the more rigorous transmission line treatment, it is apparent that $\mathcal{R}\varphi$ must be small compared with h for the lumped core and leakage reluctance approximation to be valid. If $\mathcal{R}\varphi/h$ is small, the potential drop in the core, $\mathcal{R}_c\varphi$, is small compared to the applied magnetomotive force $\mathfrak{F}$. In most ordinary electromagnets, the ratio $\mathcal{R}_c/\mathfrak{F}$ is small in the low density region. For sensitive relays with long cores of small cross-section, this is not the case, and the lumped constant treatment is correspondingly limited in accuracy, even at low densities.

At high densities, however, the core reluctance increases even in ordinary electromagnets. To use the transmission line analogy at high densities, it is necessary to express $\mathcal{R}\varphi$ in (20A) in terms of the Froehlich-

Kennelly relation described in Section 4. A solution to the resulting equations can be obtained in series form, but this solution is too complex for convenient use in engineering estimates. From this formulation of the problem, however, it is apparent that the use of lumped values of core and leakage reluctances at high densities can only be a rough approximation, as the reluctance per unit length must vary along the core, and the pattern of the leakage field and hence the leakage reluctance are no longer constant. However, in representing the core reluctance as increasing from its low density value and approaching infinity as $\varphi \to \varphi''$, the lumped approximation correctly represents the limiting conditions. It therefore provides a rough approximation to the intermediate values.

Series-Parallel Magnetic Circuit

Subject to the limitations discussed above, the magnetic circuit of most ordinary electromagnets can be represented in the form shown in Fig. 21. The core reluctance $\mathcal{R}_C$ is in series with two parallel paths: a leakage path of reluctance $\mathcal{R}_{L2}$, and an armature path of reluctance $\mathcal{R}_{02} + x/A_2$. The subscript 2 is used with the constants of this particular circuit to distinguish them from those of the simpler approximation to be discussed below. The magnetic circuit of Fig. 3 reduces to that of Fig. 21 if the reluctance $\mathcal{R}_A$ of the former is ignored, or considered as part of the reluctance $\mathcal{R}_{02}$.

The circuit reluctance $\mathcal{R}$, or $\mathcal{F}/\varphi$, can be derived from the circuit by the procedure applying to resistances in an electrical circuit, and is given by:

$$\mathcal{R} = \mathcal{R}_C + \frac{\mathcal{R}_{L2}\left(\mathcal{R}_{02} + \dfrac{x}{A_2}\right)}{\mathcal{R}_{L2} + \mathcal{R}_{02} + \dfrac{x}{A_2}}. \tag{23}$$

The evaluation of the constants of this circuit may be described with

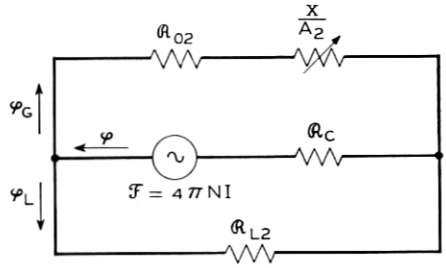

Fig. 21 — Series parallel magnetic circuit — the usual design analogy.

reference to the two structures shown schematically in Fig. 22, where Fig. 22(a) represents the familiar "end-on" armature type of construction, and Fig. 22(b) represents the "flat type" relay of Bell System use. The dashed lines indicate the path along which the length of the parts is measured, while the lined areas are those of the main, heel, and side gaps.

The core reluctance, $\mathcal{R}_C$, is determined from equation (17), taking the length as between the points 1 and 2 in both figures. The permeability is taken at the nominal maximum value throughout all iron parts.

The closed gap reluctance, $\mathcal{R}_{02}$, is the sum of the following:

A. The iron reluctance, determined from equation (17) taking the lengths of the several parts as measured around the path 2–3–4–5–6–1. In each term the cross-sectional area a is that of the part through which the flux passes. In Fig. 22(b) of course, the two side sections are added to give the total section.

B. The contact gap reluctances computed as x/a_1 and x/a_2, taking x as for an air gap of 0.005 cm. The reluctance of the joint at 1 in Fig. 22(a) is computed in the same way, and included in the sum.

C. The "stop pin" air gap reluctance, computed as x/A_2, where A_2 is the effective pole face area as determined below, and x is the separation at the measuring point for the stop pin opening.

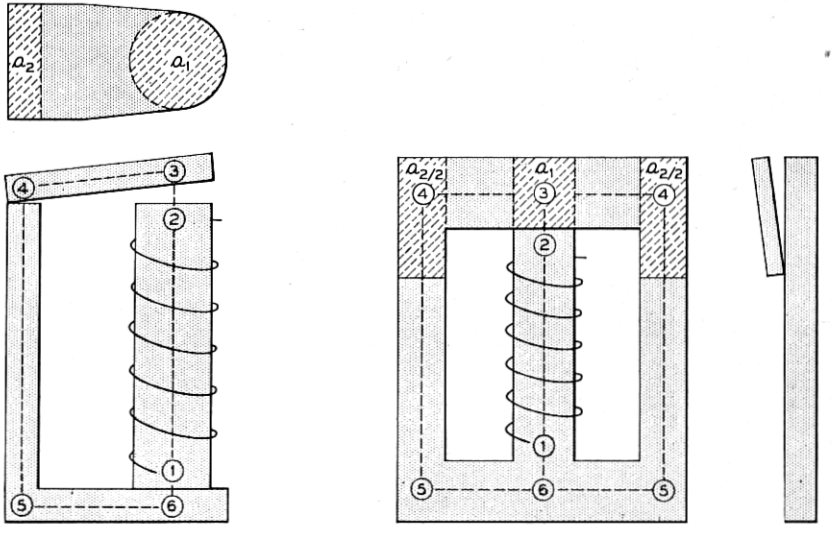

(a) END-ON ARMATURE TYPE (b) FLAT TYPE

Fig. 22 — Magnetic circuit components of typical relay structures.

The effective pole face area, A_2, is determined by equation (18), following the procedure described in the discussion of Fig. 12.

The leakage reluctance, $\mathcal{R}_{L2}$, is determined in the case of Fig. 22(a) by the procedure discussed in Section 5 and indicated in Fig. 17. In using this, ℓ_1 is the length 1–2, while ℓ_2 is the length 2–3 in Fig. 22(b) and $\ell_2 = 0$ in Fig. 22(a). The reluctance terms $C_1\ell_2$ and C_2d correspond to the armature leakage reluctance $\mathcal{R}_{LA}$ of Fig. 3, here taken as in parallel with the core leakage reluctance in determining $\mathcal{R}_{L2}$.

It should be noted that this procedure provides for two flux paths across each gap: the flux through the reluctance x/A_2, varying linearly with gap, and the parallel leakage flux through a reluctance calculated as though the armature were absent. This representation allows for the effect of fringing, taking the total field across the gap as the sum of these two fields. It carries the implication that experimentally the two fields cannot be separated by search coil measurements.

For the magnetic circuit of Fig. 21, the low density reluctance is given by equation (23). The reluctance terms are calculated for maximum permeability μ', corresponding to density B', and hence for a total core flux $\varphi' = B'a$. As discussed in Section 4, these values are approximately applicable through the low density region, or for φ less than φ'. For φ greater than φ', $\mathcal{R}_C$ is taken as given by equation (13). Thus in the high density region, the total reluctance may be written as:

$$\mathcal{R} = \mathcal{R}_C + \mathcal{R}_E,$$

where,

$$\mathcal{R}_E = \frac{\mathcal{R}_L\left(\mathcal{R}_0 + \dfrac{x}{A}\right)}{\mathcal{R}_0 + \mathcal{R}_L + \dfrac{x}{A}},$$

and,

$$\mathcal{R}_C = \mathcal{R}_C'' \frac{\varphi''}{\varphi'' - \varphi},$$

in which,

$$\mathcal{R}_C'' = \frac{\ell}{\mu' a} \cdot \frac{\varphi'' - \varphi'}{\varphi''},$$

and $\varphi'' = B''a$, where ℓ and a are the length and cross-section of the core, respectively. The values of B_M in Table I may be taken as estimates of the effective value of the saturation density B''.

Equivalent Magnetic Circuit

Over the low density region, in which the magnetic circuit reluctances are substantially independent of the flux, the expressions for the reluctance can be simplified by a procedure analogous to that used in deriving electrical network equivalents. Provided the gap reluctance varies linearly with the gap, magnetic circuits such as those of Figs. 3 and 21 can be replaced by an equivalent circuit of the simple form shown in

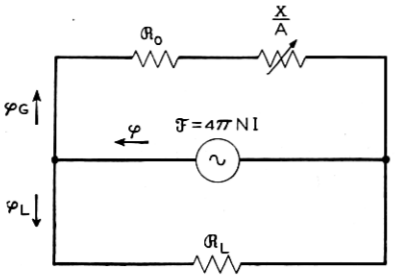

Fig. 23 — Equivalent magnetic circuit.

Fig. 23. For this simple parallel circuit, the total reluctance is given by:

$$\mathcal{R} = \frac{\mathcal{R}_L\left(\mathcal{R}_0 + \frac{x}{A}\right)}{\mathcal{R}_0 + \mathcal{R}_L + \frac{x}{A}}. \tag{24}$$

The simpler subscripts of these *equivalent* values of the magnetic circuit constants are used to distinguish them from the *design* values, applying to the magnetic circuit taken as representing the actual structure. In the usual case the design values apply to the two mesh circuit of Fig. 21, for which the additional subscript 2 is used. When a three mesh circuit is required to represent the structure, the design values are distinguished by the subscript 3, as in the constants of Fig. 3.

In the usual case in which the *design* values apply to the circuit of Fig. 21, expressions for the *equivalent* values may be obtained by comparison of the reluctance given by (23) with that given by (24). The former equation may be written in the form.

$$\mathcal{R} = \mathcal{R}_G + \mathcal{R}_{L2} - \frac{A_2\mathcal{R}_{L2}^2}{A_2\mathcal{R}_{02} + A_2\mathcal{R}_{L2} + x},$$

while (24) may be written.

$$\mathcal{R} = \mathcal{R}_L - \frac{A\mathcal{R}_L^2}{A\mathcal{R}_0 + A\mathcal{R}_L + x}.$$

By comparison, these two expressions are identical for all values of x, provided the following conditions are satisfied:

$$\mathcal{R}_L = \mathcal{R}_C + \mathcal{R}_{L2},$$
$$A\mathcal{R}_L^2 = A_2\mathcal{R}_{L2}^2,$$
$$A(\mathcal{R}_0 + \mathcal{R}_L) = A_2(\mathcal{R}_{02} + \mathcal{R}_{L2}).$$

Upon collecting terms, the relations between design and equivalent circuits are given by:

$$\begin{aligned} \mathcal{R}_L &= \mathcal{R}_C + \mathcal{R}_{L2}, \\ A &= A_2/p^2, \\ \mathcal{R}_0 &= p^2\mathcal{R}_{02} + p\mathcal{R}_C, \end{aligned} \tag{25}$$

where:

$$p = 1 + \mathcal{R}_C/\mathcal{R}_{L2}.$$

Thus the magnetization relations in the low density region can be represented by the reluctance given by (24), corresponding to the simple parallel circuit of Fig. 23, provided the constants are evaluated from those of the design circuit by means of equations (25). The evaluation of the pull and of the field energy in the low density region can therefore be conducted in terms of the simpler relations applying to the equivalent circuit.

As these simpler relations suffice to define the performance, they may be readily evaluated experimentally, using the procedures described in a companion article.[8] While these equivalent constants provide a simple and convenient means for the description and analysis of performance, they are related to the dimensions of the structure only through the conditions of equivalence given by equations (25).

Special Magnetic Circuits

The reluctance of most ordinary electromagnets can be expressed in terms of the series parallel magnetic circuit of Fig. 21, as in the two cases of Fig. 22 discussed above. Differences in configuration may affect the detailed procedure for estimating the constants, but the same circuit schematic applies. There are, however, other magnetic structures requiring different magnetic circuits for their representation. For purposes of illustration, a summary discussion of three such cases is given here.

For *armature saturation*, or cases where the flux density in the armature exceeds that of the core, as in some high speed relays, the magnetic cir-

cuit must be taken as that of Fig. 3. In this case it is the armature flux φ_A, rather than the total flux φ, which approaches a saturation value limiting the mechanical output. In the low density region, where the reluctances are constant, the conditions of equivalence given by equations (25) may be used to evaluate a simple parallel equivalent to the armature path reluctance, reducing the circuit to the form of Fig. 21, and this may in turn be reduced to an equivalent circuit of the form of Fig. 23. In the high density region, however, it is the armature rather than the core reluctance which must be expressed in terms of the Froelich-Kennelly approximation.

For *reed relays*,[6] the structural schematic is as shown in Fig. 24. In some cases, the external shield may be omitted. The magnetic circuit involves an air path through the coil in parallel with a path through the reeds. With a new interpretation of the terms, the circuit of Fig. 3 may be taken as applying, with $\mathcal{R}_C$ taken as zero, and $\mathcal{R}_{LC}$ representing the air leakage field. With some correction for the effect of the shield, this may be estimated by means of the solenoid reluctance expressions of Section 5. The controlling path is that through the reeds, represented by $\mathcal{R}_A$ for the saturating section of maximum density in series with the parallel paths between the reeds: the useful path at the gap and the leakage field. The latter may be estimated from the relations of Fig. 13.

For *polar relays*, the network contains both the permanent magnet magnetomotive force $\mathcal{F}_M$ and the coil magnetomotive force $\mathcal{F}_C$. A typical case is shown in Fig. 25. The constants applying can be evaluated by the procedures described in Section 5, and the somewhat complex circuit equations resulting can be written by the application of Kirchoff's laws in a manner wholly analogous to that for the corresponding electrical circuit.

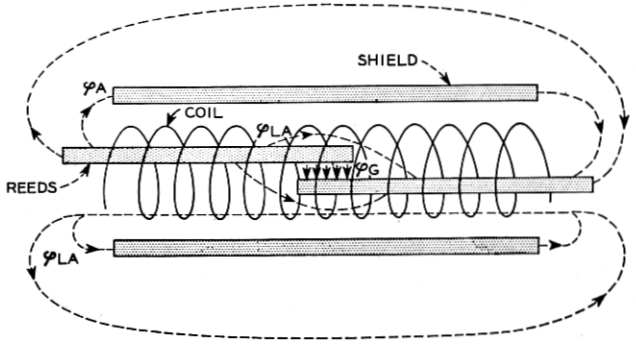

Fig. 24 — Magnetic field of a reed relay.

7 PULL EQUATIONS

Pull in Terms of Gap Flux

With the magnetization relations known, the pull can be determined from equations (7) or (8). Over the low density range, in which the magnetic circuit constants are independent of the flux, the field energy U is given by (5). Substitution of this in (7) gives the following expression for the pull F:

$$F = \frac{\varphi^2}{8\pi} \frac{d\mathfrak{R}}{dx}. \tag{26}$$

In terms of the equivalent circuit constants of Fig. 23, the reluctance $\mathfrak{R}$ is given by equation (24). Substituting this expression in (26) gives the equation:

$$F = \left(\frac{\mathfrak{R}_L}{\mathfrak{R}_0 + \mathfrak{R}_L + \dfrac{x}{A}} \right)^2 \frac{\varphi^2}{8\pi A}.$$

By comparison with (24), it can be seen that the bracketed term is the ratio $\mathfrak{R}/(\mathfrak{R}_0 + x/A)$, which equals the ratio of the gap flux to the total flux φ. Hence the preceding expression may be written in the form:

$$F = \frac{\varphi_G^2}{8\pi A} \tag{27}$$

By a parallel treatment it can be similarly shown that the application of equation (26) to the magnetic circuits of Fig. 3 and 21 gives expressions identical with (27) except that A is replaced by A_3 in the former case and by A_2 in the latter. Equation (27) is the familiar expression for

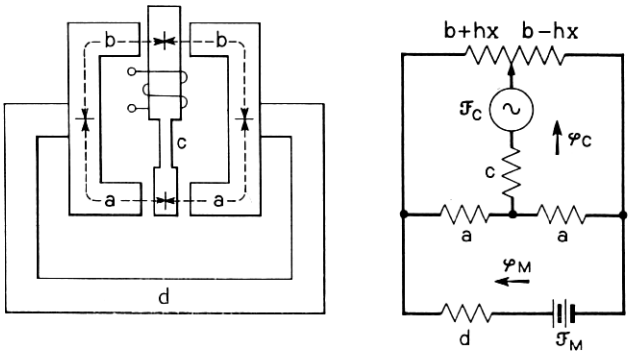

Fig. 25 — Magnetic circuit of a polar relay.

magnetic pull on two parallel planes with a field of uniform density φ_G between them. It can be directly derived from the fact that the gap energy is $\mathfrak{F}\varphi_G/(8\pi)$, with $\mathfrak{F} = x\varphi_G/A_2$. The change in this energy for a differential change dx of the gap equals $F\,dx$, so that F is given by equation (27). Derived in this way, it is apparent that (27) depends only on the field in the gap, and is quite independent of the density in the magnetic material.

Pull in Terms of Applied mmf

In the low density region, where $\mathfrak{R}$ is substantially a function of x only and the magnetization curves are linear, $W = U$, and hence the expression for F given by equation (8) becomes:

$$F = 2\pi(NI)^2 \frac{d}{dx}\left(\frac{1}{\mathfrak{R}}\right). \tag{28}$$

This expression for the pull in the linear region is known as the equation of Perrot and Picou.[9] As $NI = \mathfrak{R}\varphi/(4\pi)$, it is identical with (26).

For the magnetic circuit of Fig. 23, substitution in (28) of the expression for $\mathfrak{R}$ given by (24) gives the following expression for the pull:

$$F = \frac{2\pi(NI)^2}{A\left(\mathfrak{R}_0 + \dfrac{x}{A}\right)^2}. \tag{29}$$

In the low density region, the reluctance can always be expressed in terms of the equivalent values of Fig. 25. Using the equivalent values of closed gap reluctance $\mathfrak{R}_0$ and of pole face area A, the pull is given by equation (29). This expression is therefore of general application in the low density region, and is the most convenient equation to use for this purpose.

High Density Pull

It was shown above that equation (27) can be derived directly from the expression for the field energy associated with the gap. This expression is quite independent of the reluctance in the rest of the magnetic circuit, and is therefore equally applicable in the low and high density regions. This essentially physical argument shows that (26) and (27) are applicable through the full range of magnetization.

The same result can be obtained from equation (7) by substituting in it the expression for U given by (3), and substituting $\mathfrak{R}\varphi/(4\pi)$ for NI.

There is thus obtained:

$$F = \frac{\partial}{\partial x} \int_0^{\varphi} \frac{\mathcal{R}\varphi}{4\pi} \, d\varphi.$$

For saturation confined to the core, as in the series-parallel circuit of Fig. 21, $\mathcal{R} = \mathcal{R}_C + \mathcal{R}_E$. On substituting this expression for $\mathcal{R}$ in the preceding equation, $\mathcal{R}_C$ is independent of x and $\mathcal{R}_E$ is independent of φ, so that the expression becomes:

$$F = \frac{\varphi^2}{8\pi} \frac{d\mathcal{R}_E}{dx},$$

or, for the series parallel circuit of Fig. 21

$$F = \frac{(\mathcal{R}_{L2}\varphi)^2}{8\pi A_2 \left(\mathcal{R}_{02} + \mathcal{R}_{L2} + \frac{x}{A_2} \right)^2}. \tag{30}$$

Evidently this same expression should apply equally to the equivalent circuit of Fig. 23. That this is the case can be shown by substitution of the equivalence conditions of equations (25), giving an expression for the pull identical with (30) except that the magnetic circuit constants $\mathcal{R}_{02}$, $\mathcal{R}_{L2}$, and A_2 are replaced by their equivalent values $\mathcal{R}_0$, $\mathcal{R}_L$, and A.

Thus when saturation occurs in the core, as in most ordinary electromagnets, (30) gives the pull through the full range of magnetization, and the expression is invariant to a change from the design constants of Fig. 21 to the equivalent constants of Fig. 23. If φ is taken as φ'', the saturation flux, (30) gives the upper limit to the attainable pull. It is also useful, as shown in the companion article[1] on relay speed, in estimating the pull effective in rapid operation, when φ may be nearly constant during the latter stage of armature motion.

In estimating the steady state pull characteristics, equation (29) is applicable throughout the low density range. In the high density range, the pull may be determined from (27), or, provided saturation occurs in the core, from (30). In cases of armature saturation, the pull must be determined from (27), the expression of most general application.

8 SENSITIVITY AND WORK CAPACITY

Ampere Turn Sensitivity

Aside from any margin for rapid operation, the pull of the electromagnet must exceed the static mechanical load at all values of gap x. As illustrated in Fig. 1, this may be studied graphically by comparing

the load curve with the family of pull curves for various values of NI. The just operate ampere turn value is that for the pull curve which just exceeds the load curve at all points. For design purposes, estimated pull and load characteristics must be used in this comparison, and conditions determined for minimizing the ampere turns required to operate a specified load.

The work V done against the load is represented by the area under the load curve. Its maximum possible value is equal to the work W done by the magnet, represented by the area under the pull curve. Within the region of substantially linear magnetization, the pull is given by (29), which may be written in the form:

$$F = \frac{F_o}{(1+u)^2}, \tag{31}$$

where:

$$F_0 = \frac{2\pi(NI)^2}{A\mathcal{R}_0^2}, \tag{32}$$

and $u = x/(A\mathcal{R}_0)$, or the ratio of the gap reluctance x/A to the closed gap reluctance $\mathcal{R}_0$.

The work W done by the magnet in the travel from an initial gap x_1 to $x = 0$ is the integral of $F\,dx$, or of $A\mathcal{R}_0\,F\,du$. From (31), this integral is given by:

$$W = \frac{u_1}{1+u_1} W_{\max}, \tag{33}$$

where $u_1 = x_1/(A\mathcal{R}_0)$ and $W_{\max} = A\mathcal{R}_0 F_0$. For a large initial gap (u_1 large), W approaches $W_{\max}$, which therefore measures the upper limit to the output for this ampere turn value; the total area under the pull curve. In general, the difference between the force displacement characteristics of the load and pull curves permits only a fraction of $W_{\max}$ to be used to operate the load. The potential output of the magnet, however, depends solely upon $W_{\max}$. From (32), in which $A\mathcal{R}_0F_0$ equals $W_{\max}$, the ampere turn sensitivity, or potential output for a given ampere turn value, is given by:

$$\frac{W_{\max}}{(NI)^2} = \frac{2\pi}{\mathcal{R}_0}. \tag{34}$$

Thus the ampere turn sensitivity depends solely upon the closed gap reluctance $\mathcal{R}_0$ throughout the region of linear magnetization.

Sensitivity for Specific Loads

The part of W_{max} that can be realized depends upon the shape of the load curve. It also depends upon the travel through which the load must be moved. In principle, the latter may be adjusted to any desired value by the choice of a lever arm determining the ratio of the travel at the point of load actuation to the travel at the point where x has been measured in determining the magnetic circuit constants. The use of a lever arm linkage, of course, changes the force required, but the work V and the shape of the load characteristic remain unchanged.

In Fig. 26 is shown the pull curve relation of equation (31), together with two simple load curves: a constant load and one varying linearly with travel. In the first case, let F_1 be the constant load required, and x_1 the required travel. The pull curve to operate this load must have $F = F_1$ at $x = x_1$. Hence, from (31), $F_1/F_0 = 1/(1 + u_1)^2$. The work V_c done against the load is $F_1 x_1$, and the ratio of V_c to W_{max} is therefore $F_1 x_1/(A\mathcal{R}_0 F_0)$, or $u_1 F_1/F_0$. Hence the part of W_{max} realized against a constant load is given by:

$$\frac{V_c}{W_{max}} = \frac{u_1}{(1 + u_1)^2}. \tag{35}$$

The ratio V_c/W_{max} is shown plotted against u_1 in Fig. 27. Its maximum value is at $u_1 = 1$, where the travel $x_1 = A\mathcal{R}_0$. Maximum sensi-

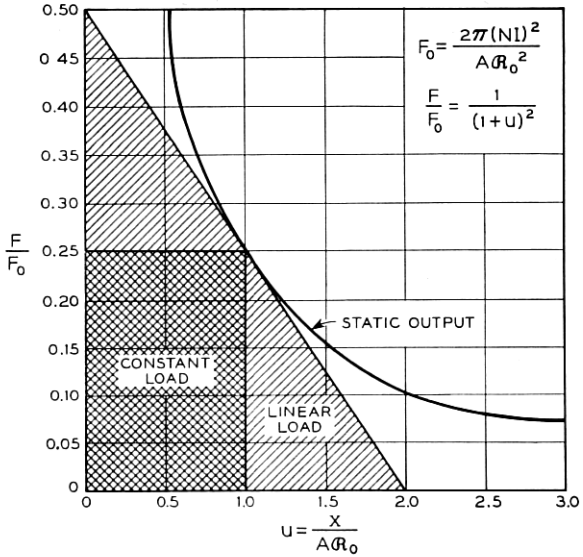

Fig. 26 — Relations between load and pull curves.

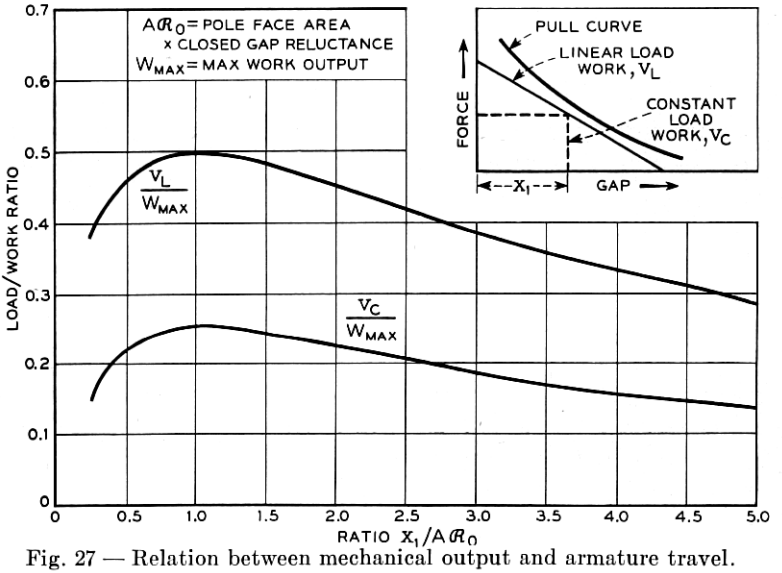

Fig. 27 — Relation between mechanical output and armature travel.

tivity is attained if the lever arm is chosen to satisfy this condition, and in this case $V_C = W_{\max}/4$.

For the case of a linear load, varying from F_2 at $x = 0$ to zero at $x = x_2$, the load is given by:

$$F = F_2\left(1 - \frac{u}{u_2}\right),$$

where $u_2 = x_2/(A\mathcal{R}_0)$. For the pull curve to be tangent to this load curve, the values of both F and dF/dx given by this last equation and by (31) must be equal at the point of tangency, x_1. These two conditions give two expressions for the ratio F_2/F_0. Equating these, there is obtained the following equation for the point of tangency:

$$u_1 = \frac{2u_2 - 1}{3} \tag{36}$$

The work done against the load is $F_2x_2/2$, and the ratio of this to $W_{\max}$ is therefore $F_2x_2/(2A\mathcal{R}_0F_0)$. Substituting the expression for F_2/F_0 obtained as described, and the expression for u_1 given by (36), there is obtained the following expression for the fraction of $W_{\max}$ realized against a linear load:

$$\frac{V_L}{W_{\max}} = \frac{(3u_1 + 1)^2}{4(u_1 + 1)^3}. \tag{37}$$

The ratio V_L/W_{max} is shown plotted against the point of tangency u_1 in Fig. 27. Its maximum value is at $u_1 = 1$, when $V_L = W_{max}/2$. For this optimum condition, $u_2 = 2$, so that the total travel, x_2, equals $2A\mathcal{R}_0$, while the point of tangency, x_1, is at half that travel. For this linear load case, under the optimum condition, the maximum work that can be usefully applied is, then, $V_L = W_{max}/2$.

Actual load curves seldom conform to either of the simple cases of Fig. 26, and more commonly have the irregular character illustrated in Fig. 1. Most of them, however, show a point of closest approach to the pull curve either at the junction of two segments, as in Fig. 28(a), or at a point of tangency to a linear segment, as in Fig. 28(b). In the former case, the coordinates of the junction point may be taken as F_1 and x_1, as indicated, and the relations for a constant load for which $V_C = F_1x_1$ applied. In the other case, the tangent segment may be extended, as indicated, to intersect the axes at F_2 and x_2, and the relations for a linear load for which $V_L = F_2x_2/2$ applied.

Quite generally, therefore, the work V done against the load curve is proportional to W_{max}, and the proportionality constant is some function of $u_1 = x_1/(A\mathcal{R}_0)$, where x_1 is the point of closest approach of the load and pull curves. Writing $f(u_1)/(2\pi)$ for the ratio V/W_{max}, it follows from equation (34) that the ampere turn sensitivity, $V/(NI)^2$ is given by:

$$\frac{V}{(NI)^2} = \frac{f(u_1)}{\mathcal{R}_0}, \tag{38}$$

where $f(u_1)$ is a maximum for $u_1 = 1$, and is similar to the curves of Fig. 27. For the particular load conditions represented by constant load

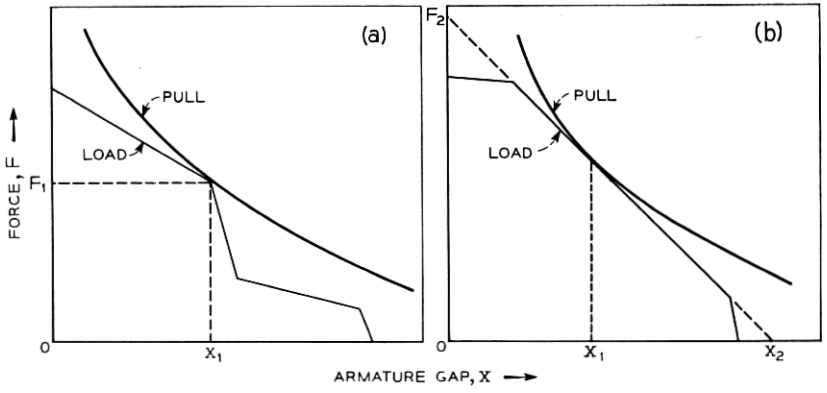

Fig. 28 — Determination of pull curve to match load.

(V_C) and linear load (V_L) characteristics, the highest values of useful work were shown to be $\pi(NI)^2/(2\mathfrak{R}_0)$, and $\pi(NI)^2/\mathfrak{R}_0$, respectively.

These relations establish the important design requirement that the point of closest approach of the load and pull curves should be at $u_1 = 1$, or where the gap reluctance x_1/A equals the closed gap reluctance $\mathfrak{R}_0$. To the extent permitted by space requirements and manufacturing considerations, this may be met by a proper choice of lever arm ratio or of pole face area. In the latter case $\mathfrak{R}_0$ is not a wholly independent parameter but includes a term varying with A, so that allowance must be made for the change in $\mathfrak{R}_0$ in changing A. The curves of Fig. 27 show that $V_C/W_{\max}$ and $V_L/W_{\max}$ decrease slowly for values of u_1 between 1 and 2. The ampere turn sensitivity is therefore close to its maximum value if u_1 lies in this range.

These relations are particularly useful in preliminary design estimates, as they permit the ampere turn requirement to be estimated for a known load merely from estimates of $\mathfrak{R}_0$ and A. For this purpose it is only necessary to determine $V/W_{\max}$ by the procedure outlined above. With V known, this determines $W_{\max}$, which equals $A\mathfrak{R}_0F_0$. Thus F_0 can be evaluated, and NI determined from equation (32).

Core Cross-Section

These relations are formally applicable only in the range of linear magnetization. For the estimates to be valid, however, it is only necessary that this condition be satisfied at the point of closest approach of load and pull curves, as an approach to saturation at smaller gaps will reduce the pull in a region where, in most cases, it is well in excess of the load curve.

For linear magnetization to obtain at the point of closest approach ($u = u_1$), the core flux should not materially exceed φ', or aB', where B' is the density for maximum permeability and a is the core cross-section. The flux is equal to $4\pi NI/\mathfrak{R}(u_1)$, and the required value of a is therefore given by:

$$a = \frac{4\pi NI}{B'\mathfrak{R}(u_1)}. \tag{39}$$

Here the values of NI and u_1 applying are those determined as described above, and $\mathfrak{R}(u_1)$ is given by equation (24) for $x = u_1A\mathfrak{R}_0$. To determine the core section a needed therefore requires an estimate of $\mathfrak{R}_L$, as well as of $\mathfrak{R}_0$ and A.

If the expression for NI given by (38) is substituted in (39), it is apparent that a varies as the square root of $V\mathfrak{R}_0/f(u_1)$ and inversely as

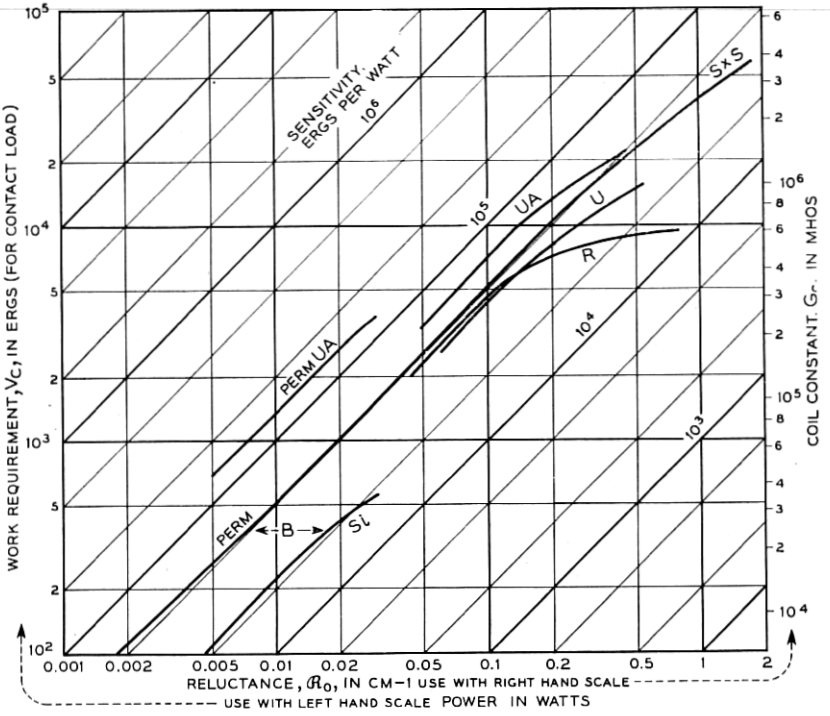

Fig. 29 — Work-power relations in terms of magnetic and coil constants.

$\mathcal{R}(u_1)$. The latter is approximately proportional to $\mathcal{R}_0$, so the core section a varies approximately as $1/\sqrt{\mathcal{R}_0}$, and hence increases with increasing ampere turn sensitivity as well as with increasing load. For values of u_1 near unity, where $f(u_1)$ is nearly constant, a decreases as u_1 increases.

Power Sensitivity

The power sensitivity is the ratio of the work V done against the load to the steady state power I^2R. From equations (1) and (38), this is given by:

$$\begin{aligned} \frac{V}{I^2R} &= G_C f(u_1)/\mathcal{R}_0 , \\ &= \frac{eS}{\rho m^2}\,\frac{f(u_1)}{\mathcal{R}_0} , \end{aligned} \tag{40}$$

where e/ρ is a constant determined by the coil construction, S is the coil volume, and m the mean length of turn. Depending on the coil depth,

the latter reflects the inside coil dimensions, which vary with the required core section a. The variation of the latter with u_1 discussed above has a minor effect on the power sensitivity, partially offsetting the effect of the term $f(u_1)$, so that $V/(NI)^2$ is nearly independent of u_1 in the range $1 \leqq u_1 \leqq 2$.

Ignoring these secondary variations, equation (40) shows that the steady state power required to operate a given load varies directly as the closed gap reluctance $\mathcal{R}_0$, and inversely as S/m^2, where S is the coil volume and m the mean length of turn. Fig. 29 shows the relationship between the work that can be done, and the steady state power that must be supplied to the coil at this time. Since, in ordinary practice, use cannot be made of the entire area under the force-deflection curve, the "constant-load work," V_C is often used in comparing magnet designs. The maximum value for this term, as determined for a number of Western Electric relays, is shown in the figure. According to equation (40) the ratio of V_C to I^2R should here have the value

$$\frac{V_C}{I^2R} = \frac{\pi G_C}{2\mathcal{R}_0},$$

since for constant-load output $f(u_1) = \pi/2$, when the optimum work condition has been chosen.

Work Capacity

In applications where maximum sensitivity is not required, higher output may be obtained by operating the electromagnet through much of its travel in the non-linear region. The controlling factor is the flux developed at the point of closest approach of the load and pull curves, so the attainable output is controlled by the pull curve for constant flux, as given by equation (30). In what follows the flux will be taken as the saturation flux φ'', corresponding to the upper limit of attainable output. The same relations may be used, however, to estimate the output attainable with any value of flux approaching φ'' in magnitude. For $\varphi = \varphi''$, (30) may be written in the form:

$$\frac{F}{F_0''} = \frac{C_L^2}{(C_L + u)^2}, \tag{41}$$

where $u = x/(A\mathcal{R}_0)$, $C_L = (\mathcal{R}_0 + \mathcal{R}_L)/\mathcal{R}_0$, and F_0'' is given by:

$$F_0'' = \frac{(C_L - 1)^2\varphi''^2}{8\pi AC_L^2}. \tag{42}$$

Equation (41) is of the same form as equation (31), with u replaced

by u/C_L, and F_0 by F_0''. Integration therefore gives an expression for the work W similar to equation (33), with u_1 replaced by u_1/C_L and W_{max}, or $A\mathcal{R}_0F_0$, replaced by $W_{sat.}$, or $C_LA\mathcal{R}_0F_0''$. There is thus obtained:

$$W = \frac{u_1}{C_L + u_1} W_{sat.} \tag{43}$$

As (43) is of the same form as (33), with u replaced by u_1/C_L, the relations between the load and pull curves are the same in the two cases. Thus the ratios $V_C/W_{sat.}$ and $V_L/W_{sat.}$ may be obtained from (35) and (37), or from Fig. 27, by using u_1/C_L to replace u. Maximum output is thus obtained when $u_1/C_L = 1$, and the gap reluctance x_1/A at the point of closest approach equals C_L. Thus the optimum leverage for maximum output differs from that for maximum sensitivity by the factor C_L.

9 DISCUSSION

Applications

The applications of the magnetization relations considered in this article are confined to the static characteristics: the sensitivity and work capacity attainable when no specific timing requirements are imposed. As the same relations control both the electrical and mechanical response of an electromagnet under dynamic as well as under static conditions, the material outlined here has further applications in other aspects of magnet performance, as illustrated in the companion articles appearing in this issue of the JOURNAL.[1,10]

The sensitivity and work capacity discussed above relate essentially to the operate characteristics. The other static characteristics of relay performance are those for release, and for marginal performance. The release characteristics are primarily dependent upon the operated load in relation to the pull at the closed gap. The rising pull characteristic as the gap is closed tends to give an operated pull well in excess of the operated load, giving a release ampere turn value small compared with the operate value. The coercive force tends to further decrease the release value, and imposes the need for stop pins to assure release. A high ratio of release to operate can be attained by providing a rising load characteristic to match the pull, by using high stop pins (thus increasing $\mathcal{R}_0$), or by using a core or armature section that saturates in the latter part of the travel. A detailed discussion of the provisions for marginal operation is outside the scope of the present article, but obviously in-

cases minor compared with that of the gaps and joints. The latter are equivalent to an air gap of 0.005 cm (2 mil-in) over the area of the joint, giving a marked advantage to one-piece construction of core and return members. The heel and main gaps necessarily introduce reluctances of similar magnitudes, further increased at the main gap by the height of the stop pins required to reduce the residual flux to the release level. It is therefore advantageous to use large areas for both heel and main gaps. When a small value of $\mathcal{R}_0$ is thus obtained, providing high sensitivity, its value is the more sensitive to variations in fit and alignment at the heel and main gaps, and high sensitivity therefore requires close tolerances on the dimensions controlling the fit of the armature to the pole pieces. Heavy section magnets tend to high sensitivity, partly because of the reduced reluctance of the magnetic members, but principally because heavy sections facilitate the provision of large areas at the gaps and joints.

As shown above, the effective pole face area is the reciprocal of the coefficient of x in the expression for the variable reluctance term. It therefore depends upon both the heel and main gaps, though the contribution from the heel gap is small when the armature is hinged there. For optimum sensitivity, or optimum work capacity, there are optimum values of the gap reluctance x_1/A as shown above, which can be obtained either by a choice of leverage to the load or by a choice of pole face area. It is preferable to attain these optima by varying the leverage, using as large a pole face area as possible, in order to make $\mathcal{R}_0$ small.

10 SUMMARY

The material given in this article provides a basis for relay design through the relationships between mechanical output and electrical input. From the indicated relations, one may find the mechanical work from a given magnet design, or find the magnetic design needed to provide a required mechanical output. Relationships for gaining optimum performance are also given.

The first step was to show that the mechanical work depends upon the field energy of the magnet, which is a consequence of the magnetomotive force provided. The magnetomotive force in turn is furnished by the electrical circuit, being determined jointly by the number of turns in the coil and the circuit resistance. The electrical output and the magnetic input were thus equated as

$$I^2R = \frac{\mathcal{F}^2}{16\pi^2 G_C},$$

where $G_c = N^2/R$, and is shown to be dependent on the coil dimensions and the conductivity of the wire in the winding.

The magnetic field energy is described by "magnetic flux" which, averaged for the entire magnet, is related to magnetomotive force through

$$\mathfrak{F} = \varphi\mathfrak{R},$$

where $\mathfrak{R}$ is an expression accounting for the dimensions and materials of the magnet and its air gaps, called "magnetic reluctance." The validity of this magnetic circuit concept is discussed at some length, leading to the proof that for many cases a very simplified "equivalent two-mesh circuit" may be used to represent the more complicated actual cases. As a result, performance may be expressed in terms of the equivalent values: $\mathfrak{R}_0$, "closed gap reluctance"; $\mathfrak{R}_L$, "leakage reluctance"; and A, "pole face area." Values for these terms may be estimated for cases of initial design (magnet synthesis), or be measured so as to characterize completed models (magnet analysis). Evaluation of reluctances of various magnetic circuit components is described, with numerous relations given for gaps and for magnetic materials, including an approximate relation covering the non-linear behavior of ferrous materials.

In terms of the magnetic circuit variables, force and work may then be expressed as

$$F = \frac{\mathfrak{F}^2}{8\pi A\mathfrak{R}_0^2} \frac{1}{(1+u)^2},$$

$$W = \frac{\mathfrak{F}^2}{8\pi\mathfrak{R}_0} \frac{u}{1+u},$$

where $u = x/A\mathfrak{R}_0$, the ratio of air gap to the product $A\mathfrak{R}_0$. It is thus found that greatest magnet output for force systems common in relays is obtained when the critical load is picked up at a gap $x_0 = A\mathfrak{R}_0$, which may be accomplished by choice of lever arm. The maximum work that may thus be considered useful, $V_{\max}$, depends somewhat on the particular load characteristic, and for the typical constant-load case, V_c, is related to ampere turns, and to power input as follows:

$$V_c/(NI)^2 = \pi/2\mathfrak{R}_0,$$

$$V_c/I^2R = \pi G_c/2\mathfrak{R}_0.$$

Greatest useful magnet output is thus seen to depend directly on G_c, the "coil constant," and inversely on $\mathfrak{R}_0$, the equivalent closed gap reluctance.

Additional cases are given permitting design relations to be extended into the saturated range for the iron.

REFERENCES

1. Estimation and Control of Operate Time of Relays, Part I — Theory, R. L. Peek, Jr., page 109 of this issue. Part II — Applications, M. A. Logan, page 144 of this issue.
2. A. C. Keller, A New General Purpose Relay for Telephone Switching Systems, B.S.T.J., **31,** p. 1023, Nov. 1952.
3. S. Evershed, Permanent Magnets in Theory and Practice, Institute of Electrical Engineers Journal (England) **58,** 1919–1920.
4. H. C. Roters, *Electromagnetic Devices*, John Wiley and Sons, New York, 1941.
5. S. P. Thompson and K. W. Moss, Proc. Physical Society of London, **21,** p. 622, 1909.
6. W. B. Ellwood, Glass Enclosed Reed Relay, Elec. Eng. **66,** p. 1104, Nov., 1947.
7. E. B. Rosa and F. W. Grover, Bulletin Bureau of Standards, No. 169, 1912.
8. R. L. Peek, Jr., Analysis of Measured Magnetization and Pull Characteristics, page 79 of this issue.
9. Perrot and Picou, Comptes Rendus, **175,** Dec. 9, 1922.
10. R. L. Peek, Jr., Principles of Slow Release Relay Design, page 187 of this issue.